2016-06-01

Carbon cycle history through the JurassicCretaceous boundary: A new global 13C stack

Watanabe, Sayaka

http://hdl.handle.net/10026.1/4782

10.1016/j.palaeo.2016.03.016
Palaeogeography, Palaeoclimatology, Palaeoecology
Elsevier BV

Please cite this article as: Price et al., Carbon cycle history through the Jurassic–Cretaceous boundary: A new global $\delta^{13}C$ stack Palaeogeogr. Palaeoclimatol. Palaeoecol. (2015), doi:10.1016/j.palaeo.2016.03.016

Carbon cycle history through the Jurassic-Cretaceous boundary: a new global $\delta^{13}C$ stack

Gregory D. Price[1], István Főzy[2], József Pálfy[3, 4]

[1]School of Geography, Earth & Environmental Sciences, Plymouth University, Drake Circus, Plymouth, PL4 8AA, United Kingdom (g.price@plymouth.ac.uk)

[2]Department of Paleontology and Geology, Hungarian Natural History Museum, POB 137, Budapest, H-1431 Hungary (fozy@nhmus.hu)

[3]Department of Physical and Applied Geology, Eötvös Loránd University, Pázmány P. sétány 1/C, Budapest, H-1117 Hungary (palfy@nhmus.hu)

[4]MTA-MTM-ELTE Research Group for Paleontology, POB 137, Budapest, H-1431 Hungary

ABSTRACT

We present new carbon and oxygen isotope curves from sections in the Bakony Mts. (Hungary), constrained by biostratigraphy and magnetostratigraphy in order to evaluate whether carbon isotopes can provide a tool to help establish and correlate the last system boundary remaining undefined in the Phanerozoic as well provide data to better understand the carbon cycle history and environmental

drivers during the Jurassic-Cretaceous interval. We observe a gentle decrease in carbon isotope values through the Late Jurassic. A pronounced shift to more positive carbon isotope values does not occur until the Valanginian, corresponding to the Weissert event. In order to place the newly obtained stable isotope data into a global context, we compiled 31 published and stratigraphically constrained carbon isotope records from the Pacific, Tethyan, Atlantic, and Boreal realms, to produce a new global $\delta^{13}C$ stack for the Late Oxfordian through Early Hauterivian interval. Our new data from Hungary is consistent with the global $\delta^{13}C$ stack. The stack reveals a steady but slow decrease in carbon isotope values until the Early Valanginian. In comparison, the Late Jurassic–Early Cretaceous $\delta^{13}C$ curve in GTS 2012 shows no slope and little variation. Aside from the well-defined Valanginian positive excursion, chemostratigraphic correlation durSchning the Jurassic–Cretaceous boundary interval is difficult, due to relatively stable $\delta^{13}C$ values, compounded by a slope which is too slight. There is no clear isotopic marker event for the system boundary. The long-term gradual change towards more negative carbon isotope values through the Jurassic-Cretaceous transition has previously been explained by increasingly oligotrophic condition and lessened primary production. However, this contradicts the reported increase in $^{87}Sr/^{86}Sr$ ratios suggesting intensification of weathering (and a decreasing contribution of non-radiogenic hydrothermal Sr) and presumably a concomitant rise in nutrient input into the oceans. The concomitant rise of modern phytoplankton groups (dinoflagellates and coccolithophores) would have also led to increased primary productivity, making the negative carbon isotope trend even more notable. We suggest that gradual oceanographic changes, more effective connections and mixing between the Tethys, Atlantic and Pacific Oceans, would have promoted a shift towards enhanced burial of isotopically heavy carbonate carbon and effective recycling of isotopically light organic matter.

These processes account for the observed long-term trend, interrupted only by the Weissert event in the Valanginian.

Keywords: Late Jurassic; Early Cretaceous; chemostratigraphy; carbonate carbon cycle history

1. Introduction

The Jurassic-Cretaceous transition is a relatively poorly understood interval in the development of the Mesozoic greenhouse world (Föllmi, 2012; Price et al., 2013). This is, in part, due to the lack of an agreed upon, chronostratigraphic framework for the Jurassic-Cretaceous boundary (Zakharov et al., 1996; Wimbledon et al., 2011; Michalík and Reháková, 2011; Guzhikov et al., 2012; Shurygin and Dzyuba, 2015). It is a time of contentious biotic changes, for which opinions have ranged from proposal of a putative mass extinction (Raup and Sepkoski, 1984) or a regional event (Hallam, 1986) or non-event (Alroy, 2008; Rogov et al., 2010). Using large taxonomic occurrence databases, several recent studies (particularly of tetrapods) have re-examined the Jurassic-Cretaceous boundary, and note a sharp decline in diversity around the Jurassic-Cretaceous boundary (Barrett et al., 2009; Mannion et al., 2011; Upchurch et al., 2011; Tennant et al., 2016). Further, the boundary interval is characterized by elevated extinction and origination rates in calcareous nannoplankton (Bown, 2005) set against a background of several calpionellid diversification events (Remane, 1986; Michalík et al., 2009) and an evolutionary rise of the modern plankton groups, notably dinoflagellates and coccolithophores (Falkowski et al., 2004). The system boundary also presents persistent stratigraphic correlation problems, which explains why the Jurassic–Cretaceous boundary is the only Phanerozoic system boundary for which a GSSP (Global Stratotype Section and Point) remains to be defined (Wimbledon, 2008; Wimbledon et al., 2011). The problems in global correlation of the Jurassic–Cretaceous boundary arise from the lack of an agreed upon biostratigraphical marker, in part related to general regression leading to marked provincialism in different fossil groups. The Tethyan based ammonite definition for the base of the Cretaceous has been the base of the Jacobi Zone (e.g., Hoedemaeker et al., 1993), although the base of which falls within the middle of relatively long sub-Boreal Preplicomphalus Zone and the Boreal Nodiger Zone. Other definitions of the Jurassic–Cretaceous boundary (see Grabowski, 2011; Wimbledon et al., 2011) include the base of Grandis ammonite Subzone, in the lower part of calpionellid Zone B, almost coinciding with the base of magnetozone M18r (Colloque sur la Crétacé inferieur, 1963) or the boundary between Grandis and Subalpina ammonite subzones, correlated with the middle part of calpionellid Zone B and the lower part of magnetozone M17r (Hoedemaeker, 1991). Due to scarcity of ammonites in many Tethyan Tithonian and Berriasian successions, calpionellids have been used as the main biostratigraphic tool in some studies (e.g., Horváth and Knauer, 1986; Blau and Grün, 1997; Houša et al., 2004; Boughdiri et al., 2006; Michalík et al., 2009; Grabowski et al., 2010a). The base of Calpionella Zone (B Zone) and the sudden appearance of a monospecific association of small, globular *Calpionella alpina* (referred to by authors as the *alpina* "acme", Remane 1985; Remane et al., 1986) is sometimes used as an indicator of the Jurassic-Cretaceous boundary. The base of reversed- polarity chron M18r has also been suggested as a convenient global correlation horizon near the clustering of these possible biostratigraphic-based boundaries (Ogg and Lowrie, 1986). The recognition of this magnetozone across provincial realms (e.g., Ogg et al., 1991; Houša et al., 2007; Grabowski et al., 2010a) has enabled inter-regional correlations. In the GTS2012, Ogg and Hinnov (2012a) utilize the base of chron M18r for assigning the numerical age (145.0 Ma) to the top of the Jurassic. Notably, the base of chron M18r which falls within the middle of the Berriasella jacobi Zone. Hence, Wimbledon et al. (2011) , tentatively suggest that several markers have the potential to help define any putative Jurassic-Cretaceous boundary.

Carbon isotope stratigraphy is useful both to help understand past global environmental and biotic change that affected carbon cycle, and as a correlation tool. For example, the GSSP for the base of the Eocene Series is defined by a negative excursion in the carbon isotope curve (Aubry et al., 2007).

To serve both purposes, Late Jurassic–Early Cretaceous carbon isotope stratigraphies have been developed extensively from pelagic sediments of the Tethys Ocean and Atlantic (e.g., Weissert and Channell, 1989; Bartolini et al., 1999; Katz et al., 2005; Tremolada et al., 2006; Michalík et al., 2009; Coimbra et al., 2009; Coimbra and Olóriz, 2012). Weissert and Channell (1989) documented how the Late Jurassic carbonate carbon isotopic composition shifts from $\delta^{13}C$ values of around 2.5‰ in the Kimmeridgian to values near 1.0‰ in the Late Tithonian–Early Berriasian. A change to lower $\delta^{13}C$ values was identified to occur within Magnetozones M18–M17 and within the B/C Calpionellid Zone (Weissert and Channell, 1989). The low $\delta^{13}C$ values of the earliest Cretaceous contrast with the more positive values obtained from the Valanginian (Lini et al., 1992; Hennig et al., 1999; Weissert et al., 1998; Duchamp-Alphonse et al., 2007; Főzy et al., 2010). Such variation has led to the idea that carbon isotopes may be useful in adding to the characterisation of the Jurassic–Cretaceous boundary (e.g., Michalík et al., 2009; Dzyuba et al., 2013; Shurygin and Dzyuba, 2015) although others (e.g., Ogg and Hinnov, 2012a) note the lack of significant geochemical markers. Changes in the Late Jurassic–Early Cretaceous carbon isotope record are interpreted to reflect decelerated global carbon cycling and ocean productivity (Weissert and Mohr, 1996) and have been variously linked to changes in sea level, aridity and temperature (e.g., Weissert and Channell, 1989; Ruffell et al., 2002a; Tremolada et al., 2006; Föllmi, 2012). Other carbon isotope records through the Jurassic–Cretaceous boundary show somewhat different trends. For example, Michalík et al. (2009) documented a minor (<0.5‰) negative excursion in the latest Jurassic (Late Tithonian), whilst some Boreal records (e.g., Žák et al., 2011) show negligible variation associated with the boundary. Dzyuba et al. (2013) reported a positive $\delta^{13}C$ shift immediately above the Jurassic–Cretaceous boundary. The significance of Jurassic–Cretaceous carbon isotope stratigraphies is underlined by correlation needs for the yet-to-be-defined GSSP.

In this study we report new carbon isotope data for the Late Jurassic–Early Cretaceous from two sections, Lókút Hill and Hárskút in Hungary (Figs. 2, 3). Both sections are well constrained by ammonite (Figs. 4, 5), belemnite (Vigh, 1984; Horváth and Knauer, 1986; Főzy, 1990) and calpionellid (Horváth and Knauer, 1986; Grabowski et al., 2010a) biostratigraphy. Magnetostratigraphy is also available for Lókút Hill (Grabowski et al., 2010a). The aim of this study is to assess whether a consistent pattern in carbon isotope variation can be established, particularly with respect to the Jurassic–Cretaceous boundary. To this end, we also developed a new global stack of carbonate $\delta^{13}C$ curves for the Jurassic–Cretaceous transition (from the Late Oxfordian to Early Hauterivian), based on the two newly obtained curves and a global compilation of 30 published curves from this interval. We use this global stack to evaluate the possible controls on carbon isotope variation (similar to the approach taken by Wendler (2013) for the Late Cretaceous) and the correlation potential of carbon isotope stratigraphy. Comparisons to a range of other climate proxies (including the oxygen isotopic composition of fossil belemnites derived from a range of low and mid Tethyan palaeolatitude sites) and environmental events is also made to help elucidate controls on the global $\delta^{13}C$ stack.

2. Geological setting

The studied Hungarian sections are situated ca. 6 km apart from each other in the southwestern part of the central Bakony Mountains (Fig. 1) that belongs to the Transdanubian Range, which in turn forms part of the Bakony Unit in the Austroalpine part of the AlCaPa terrane (Csontos and Vörös, 2004). This complex structural unit stretches from the Eastern Alps to the Western Carpathians. Its Mesozoic sedimentary succession is thought to have deposited on the southern passive margin of the Penninic ocean branch of the western Neotethys (Csontos and Vörös, 2004) (Fig.

1). In the lowermost part of the studied sections, the cherty Lókút Radiolarite Formation crops out (Figs. 2, 3). The overlying unit consists of red and yellowish, well-bedded nodular limestone (Pálihálás Limestone Formation), which passes gradually into light grey, less nodular, ammonite-rich facies (Szentivánhegy Limestone Formation). The uppermost part of both sections (Figs. 2, 3) are made up of white, thin-bedded, Biancone-type limestone (Mogyorósdomb Limestone Formation). The boundaries between these formations are gradational. A brief description of these lithostratigraphical units is given in Császár (1997). The studied section at Lókút (referred to as the hilltop section) ranges in age from the late Oxfordian to Berriasian, whereas at Hárskút (section HK-II) upper Kimmeridgian to Berriasian strata are exposed.

The entire Jurassic succession of Lókút Hill (exposed in three disjunct sections, of which the hilltop section is the youngest) is the most complete and thickest Hettangian to Tithonian succession of Transdanubian Range, deposited in a deep, pelagic environment (Galácz and Vörös, 1972). In the "horst and graben" palaeogeographic model proposed by Vörös and Galácz (1998), this locality represents a site of typical basinal deposition. The Upper Jurassic–lowermost Cretaceous strata (Fig. 2) are exposed on the southwestern edge of the top of Lókút Hill in an artificial trench (47° 12' 17" N, 17° 52' 56" E). The beds gently dip (20°) to the north. Biostratigraphic data from the Tithonian part of the section were first provided by Vigh (1984), later amended and complemented by late Oxfordian and Kimmeridgian cephalopod data by Főzy et al. (2011). In addition, Grabowski et al. (2010a) developed a calpionellid biostratigraphy and magnetostratigraphy for the Tithonian–Berriasian part of the section. Bed numbers of Grabowski et al. (2010a) are still visible, allowing correlation with these data and our isotope results.

At Hárskút, two measured Late Jurassic–Early Cretaceous sections (referred to as HK-II and HK-12) are exposed on the opposite sides of a small valley, the Közöskút Ravine (Fig. 3). In the ravine itself, a Lower to Middle Jurassic Ammonitico Rosso-type succession crops out. Studies by Fülöp et al. (1969) and Galácz (1975) established the presence of repeated gaps due to non-deposition. Within the "horst and graben" palaeogeographic model (Vörös and Galácz, 1998), these strata represent intermittent deposition on an elevated submarine high. Overlying the extremely lacunose Middle Jurassic and the cherty Lókút Radiolarite Formation, the Upper Jurassic limestone succession is more complete. The studied profile (HK-II) is a c. 10 m high natural cliff, also known as "Prédikálószék" ("Pulpit", 47° 09' 53,4" N, 17° 47' 7,36" E). It offers excellent outcrop of the fossiliferous Upper Jurassic to lowermost Cretaceous limestone units. For the uppermost Kimmeridgian–Tithonian part of the section, Főzy (1990) established an ammonite-based biostratigraphy, whereas for the Berriasian part of the same profile, calpionellid and ammonite stratigraphy was provided by Horváth and Knauer (1986). The section HK-II described in the present paper is situated a few hundred meters west of a complementary section (HK-12), which recently was subject of a detailed integrated stratigraphic study by Főzy et al. (2010), who demonstrated the Late Valanginian positive carbon isotope excursion, known as the Weissert event (Erba et al., 2004).

3. Material and methods

A substantial cephalopod fauna was collected from Lókút in 1962–1964 by a team of the Hungarian Geological Institute under the supervision of J. Fülöp. Our re-measuring and re-sampling of the section yielded additional specimens. Cephalopods of the studied section are housed in the Department of Palaeontology of the Hungarian Natural History Museum and partly in the Museum of the Hungarian Geological and Geophysical Institute. Perusal of the original documentation allowed us to accurately reconstruct the source beds of the specimens collected nearly 50 years ago and partly published by Vigh (1984). Ammonites (Figs. 4, 5) are preserved throughout both sections as internal moulds As the fauna consists of solely Mediterranean (i.e. Tethyan) elements, the ammonite biostratigraphic zonation of Enay and Geyssant (1975) and Olóriz (1978) were used. Belemnites of stratigraphical value were collected only from the Tithonian of the Lókút section.

For this study, stable isotope analyses of 165 bulk carbonate samples were taken from sections at Lókút (hilltop) and Hárskút (HK-II) (Figs. 2, 3). The average spacing of samples was ~0.15 m. Subsamples, avoiding macrofossils and sparry calcite veins, were then analysed for stable isotopes. Carbonate powders were analysed on a GV Instruments Isoprime Mass Spectrometer with a Gilson Multiflow carbonate auto-sampler at Plymouth University, using 250 to 400 micrograms of carbonate. Isotopic results were calibrated against the NBS-19 standard. Reproducibility for both $\delta^{18}O$ and $\delta^{13}C$ was better than ±0.1‰, based upon duplicate sample analyses.

4. Results

4.1. Biostratigraphy

Based on the rich and relatively well-preserved ammonite fauna which was collected bed-by-bed, high-resolution biostratigraphical subdivision of the lower, cephalopod-bearing part of the Upper Jurassic–lowermost Cretaceous section was possible (Főzy et al., 2011). Above the lowermost beds of probable Oxfordian age, a relatively complete succession of the Kimmeridgian Platynota, Strombecki, Divisum, Compsum, Cavouri and Beckeri zones was recognised, which is followed by the Tithonian Hybonotum, Darwini, Semiforme, Fallauxi, Ponti and Microcanthum zones. Representative and age-diagnostic Late Jurassic ammonites from the Lókút section are shown in Figure 4. The belemnite fauna allowed the recognition of four belemnites assemblages (TiBA-I to TiBA-IV) for the Tithonian part (Főzy et al., 2011). Range charts showing the distribution of the complete ammonoid and belemnite fauna were presented in Főzy et al. (2011).

From the Lókút section Grabowski et al. (2010a) published detailed calpionellid biostratigraphic data. Their lowermost samples analysed were assigned to the Early Tithonian Parastomiosphaera malmica Zone, whereas the overlying 3 m of the Szentivánhegy Limestone Formation belongs to the Chitinoidella Zone (Fig. 2). Two samples containing *Chitinoidellidae* together with a few specimens of *Praetintinnopsella* sp., were placed in the Praetintinnopsella Zone. Higher upsection, the remanei Subzone (or A1), and the intermedia (or A2) Subzone of the Crassicollaria Zone is identified (Grabowski et al., 2010a). The calpionellid assemblage of the next bed is mainly composed of *Calpionella alpina* and *Crassicollaria parvula* and was therefore assigned to the Early Berriasian alpina Subzone of the Calpionella Zone (Grabowski et al., 2010a). Therefore, Grabowski et al. (2010a) place the Tithonian-Berriasian boundary (and thus the Jurassic–Cretaceous boundary) at the Crassicollaria/Calpionella zonal boundary, following the criteria of Remane et al. (1986). In comparing the Lókút ammonite assemblages with calpionellid data, a general agreement is demonstrated where the data overlap. For example, the first appearance of chitinoidellids coincides with the base of the Microcanthum Zone (e.g., Benzaggagh et al., 2010).

Within the Hárskút HK-II section, the first beds above the radiolarite provided ammonites (Fig. 5) characteristic of the latest Kimmeridgian Beckeri Zone. Higher up the complete succession from the Hybonotum to the Ponti Zone was documented by Főzy (1990). Similarly to Lókút, the Upper Tithonian seems less complete, or at least not as well documented by means of ammonites. The Durangites and Microcanthum Zones could not be separated (Főzy, 1990). Although the upper part of the section yielded only very poorly preserved ammonites, Horváth and Knauer (1986) recognised all of the Mediterranean standard ammonite subzones, including the Jacobi, Grandis, Occitanica and Boissieri Zones (Fig. 3). Horváth and Knauer (1986) also recognised the presence of minor gaps on the basis of successive faunas, particularly in the Grandis Zone as well as within the Occitanica and Boissieri Zones.

The calpionellid assemblages identified by Horváth and Knauer (1986) at Hárskút (Fig. 3) allowed the recognition of the intermedia Subzone of the Crassicollaria Zone as well as the Berriasian alpina, elliptica, simplex and oblonga Subzones. Therefore, Horváth and Knauer (1986) place the Tithonian/Berriasian boundary at the Crassicollaria/Calpionella zonal boundary, following the criteria of Remane et al. (1986). In comparison with calpionellid data from Lókút, a general agreement is seen, as the same succession of calpionellid assemblages have been identified, significantly also across the Jurassic–Cretaceous boundary.

An integrated stratigraphic analysis of the overlying, higher part of the Lower Cretaceous (Berriasian–Hauterivian), exposed in the HK-12 section, was carried out by Főzy et al. (2010). They identified the Calpionella Zone at the base of the section, and a nearly complete sequence spanning the Occitanica to Boissieri ammonite zones. The overlying Lower Valanginian strata are condensed, but yielded rich assemblages from the Pertransiens and Campylotoxus zones. Stable isotope analyses revealed a well-defined positive $\delta^{13}C$ excursion in the Valanginian strata, identified as the Weissert event. These data are integrated with those reported in this study from the Tithonian and Berriasian of Hárskút HK-II section.

4.2. Calibration with magnetostratigraphy

Grabowski et al. (2010a) recently published integrated magneto- and biostratigraphies of the upper part of the Lókút section. The observed 6 reverse and 5 normal polarity intervals were correlated with magnetochrons M21r through to M18r spanning the Jurassic-Cretaceous boundary. On the basis of calpionellid biostratigraphy, Grabowski et al. (2010a), place the Jurassic–Cretaceous boundary between beds no. 44 and 45, and based on reference sections (e.g., Ogg et al., 1991; Houša et al., 2004) the boundary therefore appears in the middle part of normal polarity magnetosubzone M19n2n (Fig. 2). Consequently, Grabowski et al. (2010a), correlate the magnetic polarity intervals from the Jurassic–Cretaceous boundary down and up the section. This approach indicates that the magnetozone M19r occurs entirely within the intermedia subzone (A2) in the Upper Tithonian, which is consistent with other studies (e.g., Ogg et al., 1991). Likewise the M21n2n/M21r magnetosubzones fall within the Fallauxi Zone, in agreement with Ogg and Hinnov (2012a). For the Hárskút section no magnetostratigraphic data are available.

4.3 Stable carbon and oxygen isotope stratigraphy

Measurements of the carbon isotope composition of bulk carbonate yielded positive $\delta^{13}C$ values throughout the sections examined. At Lókút, values around 2.5‰ characterise the lower, Kimmeridgian part of the section, followed by a gradual negative shift, reaching a minimum of 0.0‰ within the Lower Berriasian. Higher up-section, a return towards more positive values up to 0.7‰ is observed. Biostratigraphic data (Vigh, 1984; Főzy et al., 2011; Grabowski et al., 2010a) together with magnetostratigraphic data (Grabowski et al., 2010a) allow us to accurately place the low point seen in the carbon isotope curve within these schemes. This minimum appears in the upper part of magnetosubzone M19n2n and towards the middle of calpionellid Zone B (i.e. the alpina Subzone) (Fig. 2). The oxygen isotope data at Lókút are more variable and range from ~ 0.0 to -3.2‰. The highest $\delta^{18}O$ values occur at the base of the section. Although showing a degree of scatter, isotope values become increasingly more negative, reaching -3.2‰ towards the top of the section.

At Hárskút (HK II), there is overall more isotopic variability (Fig. 3). Carbon isotope values of around 1.5‰ characterise the lower (Upper Kimmeridgian) part of the section, followed by a gradual negative shift, reaching a minimum of 0.9‰ within the Lower Berriasian. Following this, a return towards more positive values is once again observed. At the top of the section, carbon isotope values of 1.7‰ are recorded. The oxygen isotope data are much more variable in this section, too, and range from ~ -1.8 to 0.3‰. The most positive $\delta^{18}O$ values occur close to the base of the section and show significant scatter; oxygen isotope values become increasingly more negative towards the top of the section.

5. Discussion

5.1. Towards a new global $\delta^{13}C$ stack

In order to place the newly obtained stable isotope data from Lókút and Hárskút into a broader context, we compiled 31 published Late Jurassic-Early Cretaceous carbon isotope curves, covering the Oxfordian to Hauterivian interval (Fig. 6, Table 1). From the literature we gleaned those carbonate carbon isotope data which have adequate stratigraphic constraints, so that magneto and/or bio-chronostratigraphic calibration and correlation is possible. Reference was made to biostratigraphic schemes (e.g., Hoedemaeker, 1991; Remane, 1986; Wimbledon et al., 2011) that allow Tethyan–Boreal correlations as well as correlations to magnetostratigraphic data. All stratigraphic data were evaluated, so that the compilation of Gradstein et al. (2012) (e.g., Ogg and Hinnov, 2012a; 2012b) could be used. Hence, the top of the Jurassic is the base of chron M18r with a the numerical age of 145.0 Ma. These carbon isotope data are dominated by pelagic basinal locations, within Tethys and the Atlantic Ocean (Table 1, Fig. 7). These successions have often been focused upon because of one or more of the following: their completeness, the fine grained pelagic carbonate sediments suitable for isotope work, lack of or limited diagenesis and available biostratigraphy and/or magnetostratigraphy.

Despite the differences in amplitude and offsets in absolute $\delta^{13}C$ values, there is in general a good agreement of long-term $\delta^{13}C$ trends in all the sections compared, correlated on the basis of their biostratigraphic and/or magnetostratigraphic framework. There are similar trends in our data from Hungary compared with datasets from other Tethyan, Atlantic and Pacific locations (Weissert and Channell, 1989; Weissert and Mohr, 1996; Katz et al., 2005; Coimbra and Olóriz, 2012; Žák et al., 2011). Given the large distances between the sites (Fig. 7) it is notable that the overall shape the $\delta^{13}C$ curves are similar in some intervals. The $\delta^{13}C$ decline through the Late Jurassic and across the Jurassic–Cretaceous boundary, stable values in the Berriasian and a major Early Cretaceous positive $\delta^{13}C$ excursion, i.e. the Valanginian Weissert event, are clearly recognisable in all sections covering this interval. With respect to the isotope data from Lókút Hill (Fig. 2), the $\delta^{13}C$ decline through the Late Jurassic is distinct.

Differences in absolute values and amplitude most likely reflect a number of factors including local influences on the water chemistry such as nutrient levels and primary productivity, fluvial influences supplying isotopically lighter and more variable DIC, sediment reworking, and the varying contribution of diagenetic cements. Other differences arise potentially from low sampling resolution or analysis of poorly constrained or correlated sections. Those sections that show generally high amplitude $\delta^{13}C$ shifts (e.g., La Chambotte, eastern France) are potentially affected by a combination of sedimentology, diagenesis and the influence of varying supply of isotopically light DIC (Morales et al., 2013). As La Chambotte represents platform lagoonal and open-marine facies (Morales et al., 2013) high amplitude $\delta^{13}C$ variation is to be expected. Another noisy record is derived from the stratigraphically well constrained Kimmeridgian of the Swiss Jura (Colombié et al., 2011). Although, Colombié et al. (2011) showed that a long-term negative trend characterizes the entire Kimmeridgian interval studied (consistent for example with the Lókút section) the high-frequency changes in $\delta^{13}C$ most probably result from a mix of diagenetic and local environmental effects (Colombié et al., 2011).

Few $\delta^{13}C$ records across the Jurassic–Cretaceous boundary have been derived from organic carbon (e.g., Wortmann and Weissert, 2000; Morgans-Bell et al., 2001; Falkowski et al., 2005; Nunn et al., 2009; Hammer et al., 2012). The highly detailed curve for the Kimmeridge Clay in Dorset (Morgans-Bell et al., 2001) ends within the Lower Tithonian, but a declining trend from the Kimmeridgian to Tithonian is evident. Likewise a declining marine $\delta^{13}C_{org}$ trend is seen in DSDP site 534A data reported by Falkowski et al. (2005) from the Tithonian, before a pronounced positive event is seen associated with the Valanginian (Patton et al., 1984). Those Late Jurassic and Early Cretaceous $\delta^{13}C_{org}$ data derived from woody material and charcoal (Nunn et al., 2009, 2010; Pearce et al., 2005; Gröcke et al., 2005) also reveal a long-term decline in carbon-isotopes through the Late Jurassic and a positive Valanginian excursion closely matching the marine carbon-isotope curves. Notably a lack of data is apparent for the latest Tithonian and earliest Berriasian.

In order to separate the anomalous, the regional and the global trends, an average $\delta^{13}C_{carbonate}$ stack was developed (Fig. 8), based on the sections compared and presented here (Fig. 6). The new global $\delta^{13}C$ stack (Fig. 8) is used to visualise and identify those globally synchronous shifts in $\delta^{13}C$ that can be applied for global correlation. The $\delta^{13}C$ stack does not include any estimated or calculated average, but instead shows all data of the curves with a grey envelope indicating the range of absolute values. Using the available magnetostratigraphy and biostratigraphy as tie-points for alignment of the records, the curves were plotted onto the same scale, adjusted to the data from DSDP 534A of Tremolada et al. (2006), Bornemann and Mutterlose (2008) and Katz et al. (2005) in order to visualize similarities and differences. Some error may be incorporated here, particularly for shorter isotope records, even when combined biostratigraphy is available, as for example magnetostratigraphic resolution may be not fine enough to allow for multiple tie-points or variable sediment accumulation rates need to be estimated. Notably the data from Lókút and Hárskút do not fall outside of the stack. These data (from Lókút and Hárskút) are from a pelagic settings, consistently seen elsewhere. Although carbon isotope data from shallower marine settings (e.g., Colombié et al., 2011) also see similar trends attesting to the robustness of the carbon isotopic signal.

The stack clearly shows a decline in $\delta^{13}C$ throughout the Late Jurassic–Early Cretaceous, reaching a minimum in the Early Cretaceous in magnetochron M12, near the base of the Campylotoxus Zone (see also Weissert et al., 1998). The positive excursion in the Valanginian, (the Weissert event), is plainly evident. Our data from Hárskút (Fig. 3) clearly reveals the positive excursion in the Valanginian (see Főzy et al., 2010). The width of the grey envelope partly reflects the sampling density within the data set, and additional data could certainly modify the picture. Nevertheless, for intervals with similar data coverage, the outline of the envelope and its width may help evaluate the relative importance of and reproducibility of possible global isotopic trends. The well constrained Valanginian event contrasts with much of the earlier record, in particular the Early Tithonian, where the width of the grey envelope is larger, potentially reflecting local influences on the water chemistry, sediment reworking, diagenesis combined with stratigraphic uncertainty. Hence, aside from the well-defined Valanginian event, chemostratigraphic correlation using the $\delta^{13}C$ record from the Late Jurassic–earliest Cretaceous is challenging due to relatively stable $\delta^{13}C$ values, a broad envelope, compounded by a slope too slight.

In comparison, the composite Late Jurassic–Early Cretaceous $\delta^{13}C$ curve in GTS 2012 shows little more than the Valanginian Weissert event and slightly elevated values in the Late Tithonian (Ogg and Hinnov, 2012a; 2012b). A largely unvarying carbon isotope profile through this interval within the GTS 2012 appears at odds with the records summarized herein. The generalized curves in GTS 2012 were derived from Jenkyns et al. (2002) for the Late Jurassic and Föllmi et al. (2006) for the Early Cretaceous, the latter in turn relies solely on data reported by Emmanuel and Renard (1993) for the Berriasian and earliest Valanginian, and Hennig et al. (1999) for most of the Valanginian and earliest Hauterivian. In comparison, our compilation includes numerous other sources for a more reliable composite curve. The lack of variation through the Jurassic–Cretaceous boundary is therefore not particularly useful in adding to the characterisation of the boundary. The low point and return to more positive values seen in our data from Lókút and Hárskút appearing in the upper part of magnetosubzone M19n2n and towards the middle of calpionellid Zone B (the Alpina Subzone) (Figs. 2, 3) is not resolved in the $\delta^{13}C$ stack. Likewise, the positive Boreal $\delta^{13}C$ shift immediately above the Jurassic–Cretaceous boundary correlated to Tethyan records recorded by Dzyuba et al. (2013) is also not resolvable in the $\delta^{13}C$ stack.

5.2. Comparison and interpretation of $\delta^{13}C$ trends

Our newly obtained stable isotope data from Lókút and Hárskút (Figs. 2, 3), taken together with the $\delta^{13}C$ stack, as noted above, shows a shifts towards negative values throughout the Late Jurassic–Early Cretaceous, reaching a minimum in the Early Cretaceous. Mechanisms proposed to cause global shifts towards negative carbon isotope values include changes in productivity and organic carbon burial, increases in volcanic activity and episodic rapid methane release from gas hydrates contained in marine sediments. Large negative excursions in marine carbonate $\delta^{13}C$ are often associated with period boundaries and mass extinctions (Kump, 1991). Given the typically abrupt nature of isotope excursions related to inferred methane fluxes (e.g., Menegatti et al., 1998), this mechanism appears unlikely in the studied interval. Changes in carbon isotopes may, however, be related to ecological crises culminating in the disappearance of macro- and microfaunas. The Jurassic–Cretaceous boundary was earlier considered to be one of the major mass extinction events during the Phanerozoic (Sepkoski and Raup, 1986) with groups such as corals, brachiopods, bivalves, ammonites and fish all affected. As noted above, subsequent work has downgraded the boundary to a minor extinction event at most (Alroy, 2008). However, some recent studies have found evidence for a real diversity trough within terrestrial dinosaurs and marine reptiles (e.g., Mannion et al., 2011). The Jurassic–Cretaceous boundary interval is also characterized by significantly elevated extinction and origination rates in calcareous nannoplankton (Roth, 1987; Bown, et al., 2004; Bown, 2005; Tremolada, et al., 2006). Tremolada et al. (2006) document high abundances of late middle Tithonian oligotrophic taxa such as *Nannoconus* spp. and *Conusphaera* spp. correlating with low $\delta^{13}C$ values. Oligotrophic conditions in the Tethyan seaway have been linked to drier climates and a sea level low during the latest Jurassic (e.g., Hallam et al., 1991; Abbink et al., 2001; Ruffell et al., 2002b; Schnyder et al., 2006)(Fig. 8), reduced runoff and reduced nutrient fluxes to the oceans, lowering the fertility of surface waters (e.g., Weissert and Channell, 1989). Hence, the sea-level fall during the latest Jurassic to early Berriasian (e.g., Haq, 2014) may in part correlate with aridity, lower inputs of nutrients and the gradual negative $\delta^{13}C$ shift. A kaolinite minimum is known from all over Europe and associated with a major Late Jurassic “dry event” (e.g., Hallam et al. 1991, Abbink et al. 2001; Rameil, 2005; Schnyder et al., 2006). Rameil (2005), inferred from cyclostratigraphy, the duration of the dry phase, as defined on the Jura platform, to be 8.4 Ma (Fig. 8). However, both field observations and sedimentary log interpretation, suggest that the drier phase can be subdivided into a dry phase sensu stricto lasting about 2.8 Ma, followed by a longer transition phase (Rameil, 2005). However, the decline in $\delta^{13}C$ seen is not a short interval associated just with the Jurassic–Cretaceous boundary but one that begins in Oxfordian times and continues into the Early Valanginian. The change to once again more positive carbon isotopes in the Early Cretaceous Tethyan seaway in the Valanginian is therefore interpreted as a change to increasingly nutrient-rich conditions and enhanced carbon cycling (Weissert and Channell, 1989). The similarity of the $\delta^{13}C_{org}$ trends derived from woody material and charcoal, noted above, to the marine carbonate $\delta^{13}C$ stack clearly supports the notion that the surface ocean and atmosphere behaved as coupled reservoirs at this time.

In contrast, the Sr isotope record for this interval (Fig. 8) (e.g., Jones et al., 1994; McArthur et al., 2004; Bodin et al., 2009; Wierzbowski et al., 2012) shows a trend towards more radiogenic values from a long-term low at the Callovian-Oxfordian boundary to a peak in the Barremian. This variation in Sr-isotopes possibly reflects a change in the balance of flux from relatively non-radiogenic Sr derived from mid-ocean ridge hydrothermal activity to relatively radiogenic Sr derived from continental weathering (including changes in both total riverine flux and the isotopic composition of the flux). The $^{87}Sr/^{86}Sr$ low in the middle Oxfordian is, however, not seen as correlatable with an obvious pulse of ocean crust production (e.g., Rowley, 2002) or with the formation of a large igneous province. Wierzbowski et al., (2012) do call upon fast oceanic crust spreading and opening of new ocean basins during the Bathonian– Callovian-Oxfordian related to the breakup of Gondwana to account for the Callovian-Oxfordian minimum $^{87}Sr/^{86}Sr$ ratios observed (Fig. 8). Indeed, the data Cogné and Humler (2006) do possibly point to higher overall seafloor spreading rates for the Late Jurassic. Notably, the Paraná–Etendeka large igneous province is Valanginian-Hauterivian in age with volcanic activity starting at 134.6 ± 0.6 Ma or at 134.3 ± 0.8 Ma (Thiede and Vasconcelos, 2010; Janasi et al., 2011) coincident with the onset of the Weissert Event (Martinez et al., 2015). The Sr-isotope data at this time (Fig. 8) does not show any inflections in the curve (McArthur et al., 2001). Indeed, investigations regarding the spreading and production rates of oceanic ridges (e.g., Rowley, 2002; Cogné and Humler, 2006) show fairly constant production rates of oceanic crust during the Cretaceous. If rates of ocean floor production do not change substantially, then hydrothermal Sr fluxes should also be relatively invariant over long time scales. The implication is that the source of Sr from continental weathering is likely to be a major factor governing the evolution of marine $^{87}Sr/^{86}Sr$. Indeed, phosphorus flux rates (Föllmi, 1995) which are dependent on continental weathering rates, show a decrease from a high values in the Late Jurassic, to a low through the Jurassic–Cretaceous boundary, and a subsequent increase through into Hauterivian times. Likewise high sediment fluxes to the central North Atlantic Ocean during the latest Jurassic to Early Cretaceous (post the Late Jurassic “dry event”) are also observed (e.g., Thiede and Ehrmann, 1986). Episodes of increased hydrothermal activity are, however, not necessarily directly related to rates of ocean-crust production and phenomena as ridge jumps or changes in ridge orientation may substantially increase hydrothermal venting by additional fracturing of oceanic crust and consequent greater access of seawater to hotter, fresher material at the ridge axis (Jones and Jenkyns, 2001).

The relatively short-lived arid episode (or dry phase sensu stricto, Rameil, 2005) and possible linked short-term sea-level fall and rise (e.g., Haq, 2014) appears not to be reflected in the Sr-isotope curve. The short duration of arid conditions and presumed reduction in continental weathering and change in $^{87}Sr/^{86}Sr$ ratios, is unlikely to be resolvable over such a short timescale as inputs and outputs of Sr are possibly buffered too well by the large oceanic reservoir of Sr (Richter and Turekian, 1993). Likewise, short-term ocean fertilisation, productivity and carbon burial events, appear also not to be reflected in either the Sr-isotope or the carbon isotope curves. For example, deposition of significant petroleum source rocks of Late Jurassic and Early Cretaceous age, known from Arabian-Iranian region, West Siberia, the North Sea, Greenland Sea (Klemme and Ulmishek, 1991) and Mexico (the Casita Fm, Adatte et al., 1996) are evidently not expressed within the $\delta^{13}C$ record (Weissert and Mohr, 1996; Price and Rogov, 2009; Föllmi, 2012). Paradoxically, evidence for widespread organic matter deposition in the marine environment during the Valanginian is rather scarce, yet the Valanginian does show a pronounced positive carbon isotope excursion (e.g., Lini et al., 1992; Channell et al., 1993; Bersezio et al., 2002; Erba et al., 2004; Duchamp–Alphonse et al., 2007; Sprovieri et al., 2006; Littler et al., 2011, Figs. 6, 7). Hence simple models of transient positive carbon isotope excursions associated with burial and sequestration of isotopically light marine carbon (^{12}C) may not be fully applicable for this interval. Likewise, given the evolutionary rise of the modern plankton groups through Late Jurassic–Early Cretaceous time one would anticipate an overall increase in $\delta^{13}C$ values in marine carbonates (e.g., Falkowski et al., 2004).

The type of carbon burial (organic vs. carbonate carbon), accumulation rates, and areal distribution of facies may instead be important factors with respect to changes in the carbon isotopic signature of the Jurassic and Cretaceous oceans (Weissert, 2011; Föllmi, 2012). Mass balance models for the Cretaceous (Locklair et al., 2011) suggest that elevated rates of carbonate burial (burying relatively isotopically heavy carbon) could have dampened changes in $\delta^{13}C_{DIC}$ expected from elevated organic carbon burial rates (Weissert and Mohr, 1996; Föllmi, 2012). Indeed through the Late Jurassic-Early Cretaceous transition elevated rates of carbonate burial and preservation are observed (e.g., Mackenzie and Morse, 1992; Berner and Mackenzie, 2011). For example, during the Late Jurassic carbonate sedimentation became dominant over wide parts of the northern Tethys (Rais et al., 2007), with the expansion and development of new reef sites (Leinfelder et al., 2002; Cecca et al., 2005). Likewise, the surge of diversification of calcareous nannoplankton at the Jurassic-Cretaceous boundary interval involved the evolution of three large and heavily calcified genera that would have greatly increased the transfer and burial efficiency of carbonate (Tremolada et al., 2006). In terms of the areal distribution, widespread biogenic deep-water carbonate sedimentation (Zeebe and Westbroek, 2003) within a well-mixed ocean at this time would provide means to maintain a steady state between carbonate-mineral burial (Locklair et al., 2011) and weathering, buffering changes in carbon cycling. In contrast, earlier ocean systems (before pelagic calcifiers became increasingly abundant) were dominated by biogenic shallow-water carbonate precipitation perhaps explaining why in the Palaeozoic, Triassic and Early Jurassic carbon isotope anomalies (e.g., Payne et al., 2004; Hesselbo et al., 2007) have amplitudes of up to 6 ‰ or more.

Certainly organic carbon burial occurred during the Late Jurassic and Early Cretaceous, but within marginal seas (e.g., Wignall and Hallam, 1991; Hantzpergue et al., 1998; Price and Rogov, 2009).

Deposition in marginal seas would have been initiated as eustatic sea-level peaked in the Kimmeridgian–early Tithonian, followed by a lowstand across the Jurassic-Cretaceous boundary, followed by a slight rise, and fall again in the Valanginian–Hauterivian (Hallam, 2001; Haq, 2014) (Fig. 8). However, carbon burial within marginal seas evidently did not impact significantly on the global ocean chemistry, due to the possibly relatively small size of marginal seas compared to the global ocean and through efficient ocean mixing. Indeed, the Late Jurassic was a time of progressive fragmentation of Pangaea (Dercourt et al., 1994) and new oceanic gateways were formed and in particular, the opening of the Hispanic Corridor, connecting the Pacific to the Atlantic Ocean (Ziegler, 1988). Although the first shallow-water connection between the Tethys/Atlantic Ocean and the Pacific Ocean is dated as Pliensbachian–Toarcian (Aberhan, 2001) the continuous deepening of the Hispanic Corridor associated with a first order sea-level rise, allowed significant water mass exchange between the two basins during the Late Jurassic (Riccardi, 1991; Stille et al., 1996; Hallam, 2001, Fig. 7). Studies on reef development (Leinfelder et al., 2002) for example confirm the establishment of a first true seaway around the Callovian–Oxfordian boundary.

It has also been suggested that a decrease in organic carbon burial on the continent (Föllmi, 2012) may also have played a role in buffering the $\delta^{13}C$ record. The dominance of arid conditions on the continent (e.g., Hallam et al., 1991; Schnyder et al., 2006) may have precluded major organic carbon production and preservation. Indeed relatively large amounts of coal deposition in the earlier part of the Jurassic is followed by a decline through the Jurassic–Cretaceous boundary (e.g., Bluth and Kump 1991). Conversely, Westerman et al., (2010) and Kujau et al., (2012) for example, call for continental organic carbon burial (i.e. coal deposition) to explain the Valanginian carbon cycle perturbation. If, as noted above, the surface ocean and atmosphere behaved as coupled reservoirs at this time, this would not preclude continental organic carbon burial as a viable means to affect carbon cycling.

5.3. Oxygen isotopes and palaeoenvironmental change

The preservation of primary $\delta^{13}C$ values during carbonate diagenesis is quite typical, and is likely due to the buffering effect of carbonate carbon on the diagenetic system, as this is the largest carbon reservoir (e.g., Scholle and Arthur, 1980). Fluid-rock interactions during diagenesis, however, commonly result in a change in oxygen isotope ratios leading to relatively light $\delta^{18}O_{carb}$ values (Hudson, 1977). Hence, with respect to the oxygen isotope data, a diagenetic overprint affecting the samples analysed and results cannot be excluded. Nevertheless, the oxygen isotope data from both sites in Hungary do show a similar pattern. Furthermore, given that the isotopic trends are the same as that seen from diagenetically screened belemnites from Lókút (Főzy et al., 2011) we are confident that the trends do reflect a primary signal, independent of diagenesis. Increasingly negative $\delta^{18}O$ values are often correlated with elevated temperatures in environmental settings where continental ice volume is at a minimum and evaporation or freshwater inputs are minor factors. Similar trends have been observed elsewhere (e.g., Tremolada et al., 2006; Price and Rogov, 2009; Grabowski et al., 2010b), but not universally as other studies found opposite trends (e.g., Emmanuel and Renard, 1993; Padden et al., 2002). Larger datasets through the Late Jurassic and into the Cretaceous, based on the isotopic composition of fossil belemnites and brachiopods (e.g., Veizer, et al., 1999; Gröcke et al., 2003; Wierzbowski, 2004; McArthur et al., 2007; Riboulleau et al., 1998; Bodin et al., 2009, 2015; Price and Rogov 2009; Dera et al., 2011; Alberti et al., 2012; Price et al., 2000; 2011; 2013; Meissner et al., 2015), also show a similar trends (Fig. 8). The data compiled in Figure 7 are derived from data from a range of low and mid Tethyan palaeolatitudes and should, therefore, be less affected by regional (e.g., salinity-driven) isotopic variation. Nevertheless trends can also be linked to other factors, for example variation in terrestrial water bodies and sea level variations (e.g., Föllmi 2012). If, interpreted in terms of temperature, the data point to Oxfordian warming and a further peak in the middle Tithonian separated by a temperature plateau. Oxfordian warming and a temperature peak in the middle Tithonian is consistent with TEX_{86} temperature data of Jenkyns et al. (2012). A possible Late Berriasian cooling event is seen (a shift to more positive $\delta^{18}O$ values), followed by cooling through the Valanginian. The Hauterivian shows a return to warmer conditions. Shorter term trends through the Jurassic-Cretaceous boundary interval are less clear as belemnite oxygen isotope data in this compilation are fewer and the 95% confidence interval is greater. The scatter in values here means trends must be interpreted with caution. Notably, despite some considerable change in oxygen isotopes through the Late Jurassic and Early Cretaceous, any recognisable correlation with the $\delta^{13}C$ curve is lacking. For example, during the pronounced Valanginian shift to more positive carbon isotope values (the Weissert event), temperatures continue to fall, but as part of a longer term trend. The TEX_{86} data of Littler et al. (2011), also showed little recognisable correlation of temperature with the $\delta^{13}C$ curve for the Valanginian.

Of note is that the transition from arid to humid climates through the Late Jurassic and Early Cretaceous may have been associated with the net transfer of water to the continent owing to the infill of dried-out groundwater reservoirs in internally drained inland basins (Föllmi, 2012) and thereby affecting the oxygen isotope of seawater. The prominent Late Berriasian shift to more positive $\delta^{18}O$ values, could conceivably be related to the observed arid to humid climate transition, short-term sea-level fall (Fig. 8) and a net transfer of water towards the continent (e.g., Föllmi, 2012). Recently, Wendler et al. (2016) also demonstrated that aquifer eustasy represents a viable alternative to explain sea level fluctuations and consequently variation in the oxygen isotope of seawater.

6. Conclusions

The $\delta^{13}C$ data from Hungary are consistent with other isotope stratigraphies and indicate that the Lókút and Hárskút sections record global events, as reflected in a stack of 30 individual carbon isotope curves. Aside from the well-defined Valanginian event, chemostratigraphic correlation using the $\delta^{13}C$ record is challenging due to relatively stable $\delta^{13}C$ values showing a slope which is too slight. The Berriasian minimum and the return to more positive values seen in our data from Lókút and Hárskút is not resolved in the global $\delta^{13}C$ stack. Oxygen isotopes point to warming through the Late Jurassic interval, broadly in agreement with larger datasets through the Jurassic and Cretaceous, based on the isotopic composition of fossil belemnites and brachiopods. This latter dataset point to a stepwise cooling through the Valanginian. Notably, despite large changes in temperature through the Late Jurassic and Early Cretaceous any recognisable correlation with the $\delta^{13}C$ curve is lacking.

The Late Jurassic $\delta^{13}C$ decline has been explained by increasingly oligotrophic conditions in the Tethyan seaway (e.g., Weissert and Channell, 1989), whilst more positive carbon isotope values in the Valanginian are ascribed to increasingly nutrient-rich conditions and enhanced carbon cycling and burial. However, the Jurassic–Cretaceous boundary interval is also characterized by elevated rates of calcareous nannoplankton turnover and enhanced organic carbon deposition that it is not expressed within the $\delta^{13}C$ record. The type of carbon burial (organic vs carbonate carbon), accumulation rates, and areal distribution of facies may be the key, whereby elevated rates of carbonate burial (including large and heavily calcified calcareous nannoplankton, Tremolada et al., 2006) could have buffered changes in $\delta^{13}C_{DIC}$ expected from elevated weathering and increased organic carbon burial rates (particularly in marginal seas). We envisage also well-mixed parts of the ocean, perhaps as a result of connections established between the Tethys and Central Atlantic, and the full opening of the Hispanic Corridor effectively linking the Atlantic and Pacific Oceans. This scenario reconciles the apparently contradictory trends in carbon and strontium isotopes. The strontium isotope data through the Jurassic-Cretaceous interval points to a longer term intensification of weathering (and a decreasing contribution of non-radiogenic hydrothermal Sr), which would have presumably increased the transfer of elements such as silica and phosphorus from the continents to the oceans (e.g., Föllmi, 1995) resulting in increased productivity. An increased transfer of elements is consistent with the observation of high sediment fluxes to the central North Atlantic Ocean during the latest Jurassic to Early Cretaceous (post the Late Jurassic "dry event"). However, there is a background evolutionary rise of the modern plankton groups, notably organic-walled phytoplankton (i.e. dinoflagellates) and calcareous nannoplankton (coccolithophores) in Late Jurassic–Early Cretaceous time (Falkowski et al., 2004). Therefore the effectiveness of the biological carbon pump and export of carbonate carbon is expected to gradually increase. The carbon isotope trend is thus all the more remarkable, as its forcing counterbalances the effects of the "Mesozoic plankton revolution".

Acknowledgments

Márton Rabi (ELTE University, Budapest) is thanked for his kind assistance in the field. This work has been supported by the Hungarian Scientific Research Fund (OTKA Grant No. 68453) and received support from the SYNTHESYS Project (http://www.synthesys.info/), financed by European Community

Research Infrastructure Action under the FP6 Structuring the European Research Area Program. László Kordos (former director of the Museum of the Hungarian Geological Institute) is thanked for providing access to the fossil collections in his care. We would like to thank Claude Colombié for constructive comments on an earlier version of this paper. We thank Thierry Adatte and an anonymous reviewer for constructive and helpful reviews. This is MTA-MTM-ELTE Paleo contribution No. 218.

References

Abbink, O., Targarona, J., Brinkhuis, H., Visscher, H., 2001. Late Jurassic to earliest Cretaceous palaeoclimatic evolution of the southern North Sea. Global and Planetary Change 30, 231–256.

Aberhan, M., 2001. Bivalve palaeobiogeography and the Hispanic Corridor; time of opening and effectiveness of a proto-Atlantic seaway. Palaeogeography, Palaeoclimatology, Palaeoecology 165, 375–394

Adatte T., Stinnesbeck W., Remane, J., Hubberten, H., 1996. Paleoceanographic changes at the Jurassic–Cretaceous boundary in the Western Tethys, northeastern Mexico. Cretaceous Research 17 , 671–689.

Adatte, T., Stinnesbeck,W., Hubberten, H., Remane, J., Lopez-Oliva, J.G., 2001. Correlation of a Valanginian stable isotopic excursion in northeastern Mexico with the European Tethys. American Association of Petroleum Geologists Memoir 75, 371–388.

Alberti, M., Fürsich, F.T., Pandey, D.K., 2012. The Oxfordian stable isotope record ($\delta^{18}O$, $\delta^{13}C$) of belemnites, brachiopods, and oysters from the Kachchh Basin (western India) and its potential for palaeoecologic, palaeoclimatic, and palaeogeographic reconstructions. Palaeogeography, Palaeoclimatology, Palaeoecology 344-345, 49–68.

Alroy, J., 2008. Dynamics of origination and extinction in the marine fossil record. Proceedings of the National Academy of Sciences 105, 11536-11542.

Aubry, M.-P., Ouda, K., Dupuis, C., Berggren, W.A., Van Couvering, J.A., the Members of the Working Group on the Paleocene/Eocene Boundary, 2007. Global Standard Stratotype-section and Point (GSSP) for the base of the Eocene Series in the Dababiya Section (Egypt). Episodes 30, 271–286.

Barbu, V., 2014, alanginian isotopic and palaeoecological signals from the Bucegi Mountains, Southern Carpathians, Romania. In Bojar, A.-V., Melinte-Dobrinescu, M.C. & Smit, J. (Eds.), Isotopic Studies in Cretaceous Research. Geological Society, London, Special Publications, 382, p. 5–29.

Barrett, P.M., McGowan, A.J., Page, V., 2009. Dinosaur diversity and the rock record. Proceedings of the Royal Society of London. Series B: Biological Sciences 276, 2667–2674.

Bartolini, A., Baumgartner, P.O., Guex, J. 1999. Middle and Late Jurassic radiolarian paleoecology versus carbon isotope stratigraphy. Palaeogeography, Palaeoclimatology, Palaeoecology 145, 43–60.

Benzaggagh, M., Cecca, F., Rouqet, I., 2010. Biostratigraphic distribution of ammonites and calpionellids in the Tithonian of the internal Prerif (Msila area, Morocco). Paläontologische Zeitschrift 84, 301–315.

Berner, R.A., Mackenzie, F.T., 2011. Burial and preservation of carbonate rocks over Phanerozoic time. Aquatic Geochemistry 17, 727–733.

Bersezio, R., Erba, E., Gorza, M., Riva, A., 2002. Berriasian-Aptian black shales of the Maiolica formation (Lombardian Basin, Southern Alps, northern Italy): Local to global events. Palaeogeography, Palaeoclimatology, Palaeoecology 180, 253–275.

Blakey, R., 2015. Colorado Plateau Geosystem, Inc.TM. Accessible at: http://cpgeosystems.com/index.html. Accessed on 3rd December 2015.

Blau, J., Grün, B., 1997. Late Jurassic/Early Cretaceous revised calpionellid zonal and subzonal division and correlation with ammonite and absolute time scales. Miner. Slovaca 29, 297–300.

Bluth, G.J.S., Kump, L.R., 1991. Phanerozoic paleogeology. American Journal of Science 291, 284–308.

Bodin, S., Fiet, N., Godet, A., Matera V., Westermann, S., Clement, A., Janssen, N.M.M., Stille, P., Föllmi, K.B. 2009. Early Cretaceous (late Berriasian to early Aptian) palaeoceanographic change along the northwestern Tethyan margin (Vocontian Trough, southeastern France): $\delta^{13}C$, $\delta^{18}O$ and Sr-isotope belemnite and whole-rock records. Cretaceous Research 30, 1247–1262.

Bodin, S., Meissner, P., Janssen, N.M.M., Steuber, T., Mutterlose, J., 2015. Large igneous provinces and organic carbon burial: Controls on global temperature and continental weathering during the Early Cretaceous. Global and Planetary Change 133, 238–253.

Bornemann, A., Mutterlose, J. 2008. Calcareous nannofossil and ^{13}C records from the Early Cretaceous of the Western Atlantic Ocean: Evidence for enhanced fertilization across the Berriasian-Valanginian transition. Palaios 23, 821–832.

Bown, P.R., 2005. Calcareous nannoplankton evolution: a tale of two oceans. Micropaleontology 51, 299–308.

Bown, P.R., Lees, J.A., Young, J.R., 2004. Calcareous nannoplankton evolution and diversity through time, In: Thierstein, H.R., Young, J.R. (Eds.), Coccolithophores: From Molecular Processes to Global Impact. Springer, Berlin, pp. 481–508.

Boughdiri, M., Sallouhi, H., Maalaoui, K., Soussi, M., Cordey, F., 2006.Calpionellid zonation of the Jurassic–Cretaceous transition in north Atlasic Tunisia. Updated Upper Jurassic stratigraphy of the “Tunisian Trough” and regional correlations. Comptes Rendus Geoscience 338, 1250–1259.

Brenneke, J.C., 1978. A comparison of the stable oxygen and carbon isotope composition of Early Cretaceous and Late Jurassic carbonates from Sites 105 and 367. In Lancelot, Y., Seibold, E., et al., Initial Reports of the Deep Sea Drilling Project, 41: Washington, D.C. (U.S. Government Printing Office), p. 937-956.

Cecca, F., Martin Garin, B., Marchand, D., Lathuiliere, B., Bartolini, A., 2005. Paleoclimatic control of biogeographic and sedimentary events in Tethyan and peri-Tethyan areas during the Oxfordian (Late Jurassic). Palaeogeography, Palaeoclimatology, Palaeoecology 222,10–32.

Channell, J.E.T., Erba, E., Lini, A., 1993. Magnetostratigraphic calibation of the Late Valanginian carbon isotope event in pelagic limestones from Northern Italy and Switzerland. Earth and Planetary Science Letters 118, 145–166.

Cogné, J-P., Humler, E., 2006. Trends and rhythms in global seafloor generation rate. Geochemistry, Geophysics, Geosystems 7, Q03011, doi:10.1029/2005GC001148.

Coimbra, R., Immenhauser, A., Olóriz, F., 2009. Matrix micrite $\delta^{13}C$ and $\delta^{18}O$ reveals synsedimentary marine lithification in Upper Jurassic Ammonitico Rosso limestones (Betic Cordillera, SE Spain). Sedimentary Geology 219, 332–348.

Coimbra, R., Olóriz, F., 2012. Geochemical evidence for sediment provenance in mudstones and fossil-poor wackestones (Upper Jurassic, Majorca Island). Terra Nova 24, 437–445.

Colloque sur la Crétacé inferieur, Lyon, 1963. 1965. Bureau de Recherches Géologiques et Minières, Memoires, 34, 840 pp.

Colombié, C., Lecuyer, C., Strasser, A., 2011. Carbon-and oxygen-isotope records of palaeoenvironmental and carbonate production changes in shallow-marine carbonates (Kimmeridgian, Swiss Jura). Geological Magazine 148, 133–153.

Császár, G. (Ed.), 1997. Basic lithostratigraphic units of Hungary. Geological Institute of Hungary, Budapest, 114 pp.

Csontos, L., Vörös, A., 2004. Mesozoic plate tectonic reconstruction of the Carpathian region. Palaeogeography, Palaeoclimatology, Palaeoecology 210, 1–56.

Dera, G., Brigaud, B., Monna, F., Laffont, R., Pucéat, E., Deconinck, J.-F., Pellenard, P., Joachimski, M.M., Durlet, C., 2011. Climatic ups and downs in a disturbed Jurassic world. Geology 39, 215–218.

Dercourt, J., Fourcade, E., Cecca, F., Azema, J., Enay, R., Bassoullet, J.P. Cottereau, N., 1994. Palaeoenvironment of the Jurassic system in the Western and Central Tethys (Toarcian, Callovian, Kimmeridgian, Tithonian); an overview. Geobios 17 625–644.

Duchamp-Alphonse, S., Gardin, S., Fiet, N., Bartolini, A., Blamart, D., Pagel, M., 2007. Fertilization of the northwestern Tethys (Vocontian basin, SE France) during the Valanginian carbon isotope perturbation: evidence from calcareous nanofossils and trace element data. Palaeogeography, Palaeoclimatology, Palaeoecology 243, 132–151.

Dzyuba, O.S., Izokh, O.P., Shurygin, B.N., 2013. Carbon isotope excursions in Boreal Jurassic–Cretaceous boundary sections and their correlation potential. Palaeogeography, Palaeoclimatology, Palaeoecology 381–382, 33–46.

Emmanuel, L., Renard, M., 1993. Carbonate geochemistry (Mn, $\delta^{13}C$, $\delta^{18}O$) of the late Tithonian–Berriasian pelagic limestones of the Vocontian trough (SE France). Bulletin des Centres de Recherches Exploration-Production elf-Aquitaine 17, 205–221.

Enay, R., Geyssant, J., 1975. Faunes Tithoniques des chaines bétiques (Espagne méridionale). In: Colloque Limite Jurassique-Crétacé, Lyon-Neuchatel, 1973. Mémoire du BRGM 86, 39–55.

Erba, E., Bartolini, A., Larson, R.L., 2004. Valanginian Weissert oceanic anoxic event. Geology 32, 149–152.

Falkowski, P.G., Katz, M.E., Knoll, A.H., Quigg, A., Raven, J.A., Schofield, O., Taylor, F.J.R., 2004. The evolution of modern eukaryotic phytoplankton. Science 305, 354–360.

Falkowski, P.G., Katz, M.E., Milligan, A.J., Fennel, K., Cramer, B.S., Aubry, M.P., Berner, R.A., Novacek, M.J., Zapol, W.M., 2005, The rise of oxygen over the past 205 million years and the evolution of large placental mammals. Science 309, 2202–2204.

Föllmi, K.B., 1995. 160 m.y. record of marine sedimentary phosphorus burial: coupling of climate and continental weathering under greenhouse and icehouse conditions. Geology 23, 859–862.

Föllmi, K.B., 2012. Early Cretaceous life, climate and anoxia. Cretaceous Research 35, 230–257.

Föllmi, K.B., Godet, A., Bodin, S., Linder, P., 2006. Interactions between environmental change and shallow water carbonate buildup along the northern Tethyan margin and their impact on the Early Cretaceous carbon isotope record. Paleoceanography 21, PA4211.

Főzy, I., 1990. Ammonite succession from three upper Jurassic sections in the Bakony Mts. (Hungary). In: Comitato Centenario Raffaele Piccinini (Ed.), Atti del secondo convegno internazionale Fossili, Evoluzione, Ambiente, Pergola, pp. 323–329.

Főzy, I., Janssen, N.M.M., Price, G.D., Knauer, J., Pálfy, J., 2010. Integrated isotope and biostratigraphy of a Lower Cretaceous section from the Bakony Mountains (Transdanubian Range, Hungary): A new Tethyan record of the Weissert event. Cretaceous Research 31, 525–545.

Főzy, I., Janssen, N.M.M., Price, G.D., 2011. High-resolution ammonite, belemnite and stable isotope record from the most complete Upper Jurassic section of the Bakony Mts (Transdanubian Range, Hungary). Geologica Carpathica 62, 413–433.

Fülöp, J., Géczy, B., Konda, J., Nagy, E., 1969. Földtani kirándulás a Mecsek hegységben, a Villányi-hegységben és a Dunántúli-középhegységben. (Excursion Guide) Mediterrán Jura Kollokvium Budapest 1969, The Hungarian Geological Institute, Budapest, 68 pp.

Galácz, A., 1975. Bajóci szelvények az Északi Bakonyból. Földtani Közlöny, 105, 208–219.

Galácz, A., Vörös, A., 1972. A bakony-hegységi júra fejlődéstörténeti vázlata a főbb üledékföldtani jelenségek kiértékelése alapján. Földtani Közlöny 102, 122–135.

Geyssant, G. 1997. Tithonien. In: E. Cariou and P. Hantzpergue (coords.), Biostratigraphie du Jurasique Ouest−Européen et Méditerranéen. Zonations parallèles et distribution des invertébrés et microfossiles. Groupe Français Etude Jurassique. Bulletin du Centre de Recherches Elf Exploration−Production, Mémoir 17, 98–102.

Grabowski, J., 2011. Magnetostratigraphy of the Jurassic/Cretaceous boundary interval in the Western Tethys and its correlations with other regions: a review. Volumina Jurassica 2011, IX: 105–128.

Grabowski, J., Haas, J., Márton, E., Pszczółkowski, A., 2010a. Magneto- and biostratigraphy of the Jurassic/Cretaceous boundary in the Lókút section (Transdanubian range, Hungary). Studia Geophysica et Geodaetica 54, 1–26.

Grabowski, J., Michalík, J., Pszczółkowski, A., Lintnerová, O., 2010b. Magneto-, and isotope stratigraphy around the Jurassic/Cretaceous boundary in the Vysoká Unit (Malé Karpaty Mountains, Slovakia): correlations and tectonic implications. Geologica Carpathica 61, 309–326.

Gradstein, F., Ogg, J., Schmitz, M., Ogg, G. (Eds.), The Geologic Time Scale 2012. Elsevier, Boston, 1144 p.

Gröcke, D.R., Price, G.D., Ruffell, A.H., Mutterlose, J., Baraboshkin, E. 2003. Isotopic evidence for Late Jurassic–Early Cretaceous climate change Palaeogeography Palaeoclimatology Palaeoecology 202, 97–118.

Gröcke, D.R., Price, G.D., Robinson, S. A., Baraboshkin, E., Ruffell, A.H., & Mutterlose, J. 2005. The Valanginian (Early Cretaceous) positive carbon–isotope event recorded in terrestrial plants. Earth and Planetary Science Letters 240, 495–500.

Guzhikov, A. Y., Arkad'ev, V.V., Baraboshkin, E.Y., Bagaeva, M.I., Piskunov, V.K., Rud'ko, S. V., Perminov, V. A. & Manikin, A.G., 2012. New sedimentological, bio-, and magnetostratigraphic data on the Jurassic–Cretaceous boundary interval of Eastern Crimea (Feodosiya). Stratigraphy and Geological Correlation 20, 261–294.

Hallam, A., 1986. The Pliensbachian and Tithonian extinction events. Nature 319, 765–768.

Hallam, A., 2001. A review of the broad pattern of Jurassic sea-level changes and their possible causes in the light of current knowledge. Palaeogeography, Palaeoclimatology, Palaeoecology 167, 23–37.

Hallam, A., Grose, J.A., Ruffell, A.H., 1991. Palaeoclimatic significance of changes in clay mineralogy across the Jurassic–Cretaceous boundary in England and France. Palaeogeography, Palaeoclimatology, Palaeoecology 81, 173–187.

Hantzpergue, P., Baudin, F., Mitta, V., Olferiev, A., Zakharov, V.A., 1998. The Upper Jurassic of the Volga basin: ammonite biostratigraphy and occurrence of organic carbon rich facies. Correlations between boreal–subboreal and submediterranean provinces. In: Crasquin-Soleau, S., Barrier, É. (Eds.), Peri-Tethys Memoir 4: Epicratonic Basins of Peri-Tethyan Platforms. In: Mém. Mus. Natl. Hist. Nat. 179, 9–33.

Hammer, Ø., Collignon, M., Nakrem, H.A., 2012 Organic carbon isotope chemostratigraphy and cyclostratigraphy in the Volgian of Svalbard. Norwegian Journal of Geology 92, 103–112.

Haq, B.U., 2014. Cretaceous eustasy revisited. Global and Planetary Change 113, 44–58.

Hennig, S., Weissert, H., Bulot, L., 1999. C-isotope stratigraphy, a calibration tool between ammonite- and magnetostratigraphy: the Valanginian-Hauterivian transition. Geologica Carpathica 50, 91–96.

Hesselbo, S.P., Jenkyns, H.C., Duarte, L.V., Oliveira, L.C.V. 2007. Carbon-isotope record of the Early Jurassic (Toarcian) Oceanic Anoxic Event from fossil wood and marine carbonate (Lusitanian Basin, Portugal). Earth and Planetary Science Letters 253, 455–470.

Hoedemaeker P.J., 1991, Tethyan–Boreal correlations and the Jurassic–Cretaceous boundary. Newsletters on Stratigraphy 25, 37–60.

Hoedemaeker, P.J., Company, M.R., Aguirre Urreta, M.B., Avram, E., Bogdanova, T.N., Bujtor, L., Bulot, L., Cecca, F., Delanoy, G., Etiachfini, M., Memmi, L., Owen, H.G., Rawson, P.F., Sandoval, J., Tavera, J.M., Thieuloy, L.P., Tovbina, S.Z., Vasıcek, Z., 1993. Ammonite zonation for the lower Cretaceous of the Mediterranean region, basis for the stratigraphic correlation within IGCP Project 262. Revista Espanola de Paleontologia 8, 117–120.

Horváth, A., Knauer, J., 1986. Biostratigraphy of the Jurassic-Cretaceous boundary beds in the profile Közöskút Ravine II at Hárskút. Acta Geol. Hung. 29, 1–2, 65–87.

Houša, V., Krs, M., Man, O., Pruner, P., Venhodová, D., Cecca, F., Nardi G., Piscitello, M., 2004. Combined magnetostratigraphic, palaeomagnetic and calpionellid investigations across the Jurassic/Cretaceous boundary strata in the Bosso Valley, Umbria, central Italy. Cretaceous Research 25, 771−785.

Hudson, J.D., 1977. Stable isotopes and limestone lithification. J. Geol. Soc. London 133, 637–660.

Jach, R., Djerić, N., Goričan, S., Reháková D., 2014 Integrated stratigraphy of the Middle–Upper Jurassic of the Krížna Nappe, Tatra Mountains. Annales Aocietatis Geologorum Poloniae, 84, 1–33.

Janasi, V.A., de Freitas, V.A., Heaman, L.H., 2011. The onset of flood basalt volcanism, Northern Paraná, Brazil: a precise U–Pb baddeleyite/zircon age for a Chapecó-type dacite. Earth and Planetary Science Letters 302, 147–153.

Jenkyns, H.C., Jones, C.E., Gröcke, D.R., Hesselbo, S.P., Parkinson, D.N., 2002. Chemostratigraphy of the Jurassic System: applications, limitations, and implications for paleoceanography. Journal of the Geological Society, London 159, 351–378.

Jenkyns, H.C., Schouten-Huibers, L., Schouten, S., Sinninghe Damsté, J. S., 2012. Warm Middle Jurassic–Early Cretaceous high-latitude sea-surface temperatures from the Southern Ocean. Climates of the Past 8, 215–226.

Jones, C.E., Jenkyns, H.C., Coe, A.L., Hesselbo, S.P., 1994. Strontium isotopic variations in Jurassic and Cretaceous seawater. Geochim. Cosmochim. Acta 58, 3061–3074.

Jones, C.E., Jenkyns, H.C. 2001. Seawater strontium isotopes, oceanic anoxic events, and seafloor hydrothermal activity in the Jurassic and Cretaceous. American Journal of Science 301, 112–149.

Katz, M.E., Wright, J.D., Miller, K.G., Cramer, B.S., Fennel, K., Falkowski, P.G., 2005. Biological overprint of the geological carbon cycle. Marine Geology 217, 323–338.

Klemme, H.D., Ulmishek, G.F., 1991. Effective petroleum source rocks of the world: stratigraphic distribution and controlling depositional factors. American Association of Petroleum Geologists Bulletin, 75, 1809–1851.

Kujau, A., Heimhofer, U., Ostertag-Henning, C., Gréselle, B., Mutterlose, J., 2012. No evidence for anoxia during the Valanginian carbon isotope event. — An organic-geochemical study from the Vocontian Basin, SE France. Global and Planetary Change 92–93, 92–104.

Kump, L.R., 1991. Interpreting carbon-isotope excursions: Strangelove oceans. Geology 19, 299–302.

Leinfelder, R.R., Schmid, D.U., Nose, M., Werner, W., 2002. Jurassic reef patterns; the expression of a changing globe. In: Kiessling, W., Fluegel, E., Golonka, J. (Eds.), Phanerozoic Reef Patterns. Soc. Sediment. Geol. SEPM, Tulsa, US. 72, p. 465–520.

Lini, A., Weissert, H., Erba, E., 1992. The Valanginian carbon isotope event: A first episode of greenhouse climate conditions during the Cretaceous. Terra Nova 4, 374–384.

Littler, K., Robinson, S.A., Bown, P.R., Nederbragt, A.J., Pancost, R.D., 2011. High sea-surface temperatures during the Early Cretaceous Epoch, Nature Geoscience 4, 169–172.

Locklair, R., Sageman, B., Lerman, A., 2011. Marine carbon burial flux and the carbon isotope record of Late Cretaceous (Coniacian-Santonian) Oceanic Anoxic Event III. Sedimentary Geology 235, 38–49.

Lukeneder, A., Halásová, E., Kroh, A., Mayrhofer, S., Pruner, P., Reháková, D., Schnabl, P., Sprovieri, M., Wagreich, M. 2010. High resolution stratigraphy of the Jurassic-Cretaceous boundary interval in the Gresten Klippenbelt (Austria). Geologica Carpathica 61, 365–381.

Mackenzie, F.T., Morse, J.W., 1992. Sedimentary carbonates through Phanerozoic time. Geochim. Cosmochim. Acta 56, 3281–3295.

Mannion, P.D., Upchurch, P., Carrano, M.T., Barrett, P.M., 2011. Testing the effect of the rock record on diversity: a multidisciplinary approach to elucidating the generic richness of sauropodomorph dinosaurs through time. Biological Reviews 86, 157–181.

Martinez, M., Deconinck J-F., Pellenard, p., Riquier, L., Company, M., Reboulet, S., Moiroud, M., 2015. Astrochronology of the Valanginian–Hauterivian stages (Early Cretaceous): Chronological relationships between the Paraná–Etendeka large igneous province and the Weissert and the Faraoni events. Global and Planetary Change 131, 158–173.

McArthur, J.M., Howarth, R.J., Bailey, T.R., 2001. Strontium isotope stratigraphy: LOWESS Version 3. Best-fit line to the marine Sr-isotope curve for 0 to 509 Ma and accompanying look-up table for deriving numerical age. Journal of Geology 109, 155–908.

McArthur, J.M., Mutterlose, J., Price, G.D., Rawson, P.F., Ruffell, A.H., Thirlwall, M.F., 2004. Belemnites of Valanginian, Hauterivian and Barremian age: Sr-isotope stratigraphy, composition ($^{87}Sr/^{86}Sr$, $\delta^{13}C$, $\delta^{18}O$,Na, Sr, Mg), and palaeo-oceanography. Palaeogeography, Palaeoclimatology, Palaeoecology 202, 253–272.

McArthur, J.M., Janssen, N.M.M., Reboulet, S., Leng, M.J., Thirlwall, M.F., van de Schootbrugge, B., 2007. Palaeotemperatures, polar ice-volume, and isotope stratigraphy (Mg/Ca, $\delta^{18}O$, $\delta^{13}C$, $^{87}Sr/^{86}Sr$): The Early Cretaceous (Berriasian, Valanginian, Hauterivian). Palaeogeography, Palaeoclimatology, Palaeoecology 248 (3-4), 391–430.

Meissner, P., Mutterlose, J., Bodin, S., 2015. Latitudinal temperature trends in the northern hemisphere during the Early Cretaceous (Valanginian–Hauterivian). Palaeogeography Palaeoclimatology Palaeoecology 424, 17–39.

Menegatti, A.P., Weissert, H., Brown, R.S., Tyson, R.V., Farrimond, P., Strasser, A., Caron, M., 1998. High-resolution δ13C stratigraphy through the early Aptian “Livello Selli” of the Alpine Tethys. Paleoceanography 13, 530–545.

Michalík, J., Reháková, D., 2011, Possible markers of the Jurassic/Cretaceous boundary in the Mediterranean Tethys: A review and state of art. Geoscience Frontiers 2, 475–490.

Michalík, J., Reháková, D., Halásová, E., Lintnerová, O., 2009. The Brodno section – a potential regional stratotype of the Jurassic/Cretaceous boundary (Western Carpathians). Geologica Carpathica 60, 213–232.

Morales, C., Gardin, S., Schnyder, J., Spangenberg, J., Arnaud-Vanneau, A., Arnaud, H., Adatte, T., Föllmi, K.B., 2013. Berriasian and early Valanginian environmental change along a transect from the Jura Platform to the Vocontian Basin. Sedimentology 60, 36–63.

Morgans-Bell, H.S., Coe, A., Hesselbo, S.P., Jenkyns, H.C., Weedon, G.P., Marshall, J.E.A., Tyson, R.V., Williams, C.J. 2001, Integrated stratigraphy of the Kimmeridge Clay Formation (Upper Jurassic) based on exposures and boreholes in south Dorset, UK. Geological Magazine 138, 511–539.

Nunn, E.V., Price, G.D., Hart, M.B., Page, K.N., Leng, M.J. 2009, Isotopic signals from Callovian-Kimmeridgian (Middle-Upper Jurasevensic) belemnites and bulk organic carbon, Staffin Bay, Isle of Skye, Scotland. Journal of the Geological Society, London 166, 633–641. 16.

Nunn, E.V., Price, G.D., Gröcke, D.R., Baraboshkin, E.Y., Leng, M.J., Hart, M.B. 2010. The Valanginian positive carbon isotope event in Arctic Russia: evidence from terrestrial and marine isotope records and implications for global carbon cycling. Cretaceous Research 31, 577–592.

Ogg, J.G., Lowrie, W. 1986, Magnetostratigraphy of the Jurassic/Cretaceous boundary. Geology 14, 547–550.

Ogg, J.G., Hasenyager, R.W., Wimbledon, W.A., Channell, J.E.T., Bralower, T.J., 1991. Magnetostratigraphy of the Jurassic-Cretaceous boundary interval-Tethyan and English faunal realms. Cretaceous Research 12, 455−482.

Ogg, J.G., Hinnov, L.A., 2012a. Chapter 26 – Jurassic. In: Gradstein, F., Ogg, J., Schmitz, M., Ogg, G. (Eds.), The Geologic Time Scale 2012. Elsevier, Boston, pp. 731–791.

Ogg, J.G., Hinnov, L.A., 2012b. Chapter 27 – Cretaceous. In: Gradstein, F., Ogg, J., Schmitz, M., Ogg, G. (Eds.), The Geologic Time Scale 2012. Elsevier, Boston, pp. 793–853.

Olóriz, F., 1978. Kimmeridgiense-Tithónico inferior en el Sector Central de las Cordilleras Béticas (Zona Subbética). Paleontología. Bioestratigrafía. Ph.D. Thesis (1976), Tesis Doct. Univ. Granada 184, 758 pp.

Padden, M., Weissert, H., Funk, H., Schneider, S., Gansner, C., 2002. Late Jurassic lithological evolution and carbon-isotope stratigraphy of the western Tethys. Eclogae Geol. Helv. 95, 333–346.

Patton, J.W., Choquette, P.W., Guennel, G.K., Kaltenback, A.J. and Moore, A., 1984. Organic geochemistry and sedimentology of lower to mid-Cretaceous deep-sea carbonates, sites 535 and 540, Leg 77. Init. Rep. Deep Sea Drill. Proj., 77, 417–443.

Payne, J.L., Lehrmann, D.J., Wei, J., Orchard, M.J., Schrag, D.P., Knoll, A.H., 2004. Large perturbations of the carbon cycle during recovery from the end-Permian extinction. Science 305, 506–509.

Pearce, C.R., Hesselbo, S.P., Coe, A.L., 2005. The mid-Oxfordian (Late Jurassic) positive carbon-isotope excursion recognised from fossil wood in the British Isles. Palaeogeography, Palaeoclimatology, Palaeoecology 221, 343–357.

Price, G.D., Mutterlose, J., 2004. Isotopic signals from late Jurassic–early Cretaceous (Volgian–Valanginian) sub-Arctic belemnites, Yatria River, Western Siberia. Journal of the Geological Society, London 161, 959–968.

Price, G.D., Rogov, M., 2009. An isotopic appraisal of the Late Jurassic greenhouse phase in the Russian Platform. Palaeogeography, Palaeoclimatology, Palaeoecology 273, 41–49.

Price, G.D., Ruffell, A.H., Jones, C.E., Kalin, R.M.,Mutterlose, J. 2000. Isotopic evidence for temperature variation during the early Cretaceous (late Ryazanian–mid Hauterivian). Journal of the Geological Society, London 157, 335–343.

Price, G.D., Főzy, I, Janssen, N.M.M., Palfy, J. 2011. Late Valanginian–Barremian (Early Cretaceous) paleotemperatures inferred from belemnite stable isotopes and Mg/Ca ratios from Bersek Quarry (Gerecse Mountains, Transdanubian Range, Hungary. Palaeogeography, Palaeoclimatology, Palaeoecology 305, 1–9.

Price, G.D., Twitchett, R.J., Wheeley, J.R., Buono, G., 2013. Isotopic evidence for long term warmth in the Mesozoic. Scientific Reports 3, doi:10.1038/srep01438.

Rais, P., Louis-Schmid, B., Bernasconi, S.M., Weissert, H. 2007. Palaeoceanographic and palaeoclimatic reorganization around the Middle–Late Jurassic transition. Palaeogeography, Palaeoclimatology, Palaeoecology 251, 527–546.

Rameil, N., 2005. Carbonate sedimentology, sequence stratigraphy, and cyclostratigraphy of the Tithonian in the Swiss and French Jura Mountains: a high-resolution record of changes in sea level and climate. GeoFocus 13, 246 pp.

Raup, D.M., Sepkoski, J.J., Jr., 1984. Periodicity of extinctions in the geologic past. Proceedings of the National Academy of Sciences 81, 801–805.

Remane J., 1986. Calpionellids and the Jurassic-Cretaceous boundary. Acta Geologica Hungarica 29, 15–26.

Remane, J., Borza, K., Nagy, I., Bakalova-Ivanova, D., Knauer, J., Pop, G., Tardi-Filacz, E., 1986. Agreement on the subdivision of the standard calpionellid zones defined at the 2nd Planktonic Conference, Roma 1970. Acta Geologica Hungarica 29, 5–14.

Riboulleau, A., Baudin, F., Daux, V., Hantzpergue, P., Renard, M., Zakharov, V., 1998. Évolution de la paléotempérature de eaux de la plate-forme russe au cours du Jurassique supérieur. Comptes Rendus de l'Académie des Sciences Série II 326, 239–246.

Riccardi, A.C., 1991. Jurassic and Cretaceous marine connections between the Southeast Pacific and Tethys. In: Channell J.E.T., Winterer E.L., Jansa L.F. (Eds.), Palaeogeography and Paleoceanography of Tethys, p. 155–189.

Richter, F.M., Turekian, K.K., 1993. Simple models for the geochemical response of the ocean to climatic andtectonic forcing. Earth and Planetary Science Letters 119, 121–131.

Rogov, M., Zakharov, V., Nikitenko, B., 2010. The Jurassic-Cretaceous Boundary Problem and the Myth on J/K Boundary Extinction. Earth Science Frontiers 17, 13–14.

Roth, P.H., 1987. Mesozoic calcareous nannofossil evolution: relation to paleoceanographic events. Paleoceanography 2, 601–611.

Rowley, D.B., 2002. Rate of plate creation and destruction: 180 Ma to present. Geological Society of America Bulletin 114, 927–933.

Ruffell, A.H., Price, G.D., Mutterlose, J., Kessels, K., Baraboshkin, E., Gröcke, D.R., 2002a. Palaeoenvironmental sensitivity of clay minerals, stable isotopes and calcareous nannofossils: evidence for palaeoclimatic change during the Late Jurassic–Early Cretaceous, Volga Basin, SE Russia. Geological Journal 37, 17–33.

Ruffell, A.H., McKinley, J.M., Worden, R.H., 2002b, Comparison of clay mineral stratigraphy to other proxy palaeoclimate indicators in the Mesozoic of NW Europe. Philosophical Transactions of the Royal Society A., 360, 675–693.

Schnyder, J., Ruffell, A., Deconinck, J.-F., Baudin, F., 2006. Conjunctive use of spectral gamma-ray logs and clay mineralogy in defining late Jurassic–early Cretaceous palaeoclimate change (Dorset, U.K.). Palaeogeography, Palaeoclimatology, Palaeoecology 229, 303–320.

Scholle, P.A., Arthur, M.A., 1980. Carbon isotope fluctuations in Cretaceous pelagic limestones: potential stratigraphic and petroleum exploration tool. American Association of Petroleum Geologists Bulletin 64, 67–87.

Sepkoski, J.J., Jr., Raup, D.M., 1986. Periodicity in marine extinction events, In: Elliott, D.K. (Ed.), Dynamics of Extinction. John Wiley and Sons, New York, pp. 3–46.

Shurygin, B.N., Dzyuba, O.S., 2015. The Jurassic/Cretaceous boundary in northern Siberia and Boreal–Tethyan correlation of the boundary beds. Russian Geology and Geophysics 56, 652–662.

Sprovieri, M., Coccioni, R., Lirer, F., Pelosi, N., Lozar F., 2006. Orbital tuning of a lower Cretaceous composite record (Maiolica Formation, central Italy), Paleoceanography 21, PA4212, doi:10.1029/2005PA001224.

Stille, P., Steinmann, M., Riggs, S.R., 1996. Nd isotope evidence for the evolution of the paleocurrents in the Atlantic and Tethys oceans during the past 180 Ma. Earth and Planetary Science Letters 144, 9–19.

Tennant, J.P., Mannion, P.D., Upchurch, P., Sutton, M.D., Price, G.D., 2016. Biotic and environmental dynamics through the Late Jurassic–Early Cretaceous transition: evidence for protracted faunal and ecological turnover. Biological Reviews doi: 10.1111/brv.12255

Thiede, D.S., Vasconcelos, P.M., 2010. Paraná flood basalts: rapid extrusion hypothesis confirmed by new $^{40}Ar/^{39}Ar$ results. Geology 38, 747–750.

Thiede, J., Ehrmann, W.U., 1986. Late Mesozoic and Cenozoic sediment flux to the central North Atlantic Ocean. in North Atlantic Palaeoceanography, edited by C.P. Summerhayes and N.J.Shackleton, pp. 3-15, Blackwell Science.

Tremolada, F., Bornemann, A., Bralower, T., Koeberl, C., van de Schootbrugge, B., 2006. Paleoceanographic changes across the Jurassic/Cretaceous boundary: the calcareous phytoplankton response. Earth and Planetary Science Letters 241, 361–742.

Upchurch, P., Mannion, P.D., Benson, R.B.J., Butler, R.J., Carrano, M.T., 2011. Geological and anthropogenic controls on the sampling of the terrestrial fossils record: a case study from the Dinosauria. In Comparing the Geological and Fossil Records: In: McGowan, A.J., Smith A.B., (Eds.), Implications for Biodiversity Studies, Geological Society of London, Special Publication, London.pp. 209–240.

Veizer, J., Ala, D., Azmy, K., Bruckschen, P., Buhl, D., Bruhn, F., Carden, G.A.F., Diener, A., Ebneth, S., Goddéris, Y., Jasper, T., Korte, C., Pawellek, F., Podlaha, O.G., Strauss, H., 1999. $^{87}Sr/^{86}Sr$, $\delta^{13}C$ and $\delta^{18}O$ evolution of Phanerozoic seawater. Chemical Geology 161, 59–88.

Vigh, G., 1984. Die biostratigraphische Auswertung einiger Ammoniten-Faunen aus dem Tithon des Bakonygebirges sowie aus dem Tithon-Berrias des Gerecsegebirges. Annales Instituti Geologici Publici Hungarici 67, 1–210.

Vörös, A., Galácz, A., 1998. Jurassic palaeogeography of the Transdanubian Central Range (Hungary). Rivista ltaliana di Paleontológia e Stratigrafia 104, 69–84.

Weissert, H., 2011. Mesozoic Pelagic Sediments: Archives for Ocean and Climate History during Green-House Conditions In: Hüneke, H., Mulder, T., (Eds.), Deep-Sea Sediments pp. 765–792.

Weissert, H., Channell, J.E.T., 1989. Tethyan carbonate carbon isotope stratigraphy across the Jurassic-Cretaceous boundary: an indicator of decelerated carbon cycling. Paleoceanography 4, 483–494.

Weissert, H., Mohr, H., 1996. Late Jurassic climate and its impact on carbon cycling. Palaeogeography, Palaeoclimatology, Palaeoecology 122, 27–43.

Weissert, H., Lini, A., Föllmi, K.B., Kuhn, O., 1998. Correlation of Early Cretaceous carbon isotope stratigraphy and platform drowning events: a possible link? Palaeogeography, Palaeoclimatology, Palaeoecology 137, 189–203.

Wendler, I., 2013. A critical evaluation of carbon isotope stratigraphy and biostratigraphic implications for Late Cretaceous global correlation. Earth Science Reviews 126, 116–146.

Wendler, J.E., Wendler, I., Vogt, C., Kuss, J., 2016. Link between cyclic eustatic sea-level change and continental weathering: Evidence for aquifer-eustasy in the Cretaceous. Palaeogeography, Palaeoclimatology, Palaeoecology 441, 430–437.

Wierzbowski, H., 2004. Carbon and oxygen isotope composition of Oxfordian–EarlyKimmeridgian belemnite rostra: palaeoenvironmental implications for Late Jurassic seas. Palaeogeography, Palaeoclimatology, Palaeoecology 203, 153–168.

Westermann, S., Föllmi, K.B., Adatte, T., Matera, V., Schnyder, J., Fleitmann, D., Fiet, N., Ploch, I., Duchamp-Alphonse, S., 2010. The Valanginian $\delta^{13}C$ excursion may not be an expression of a global anoxic event. Earth and Planetary Science Letters 290, 118–131.

Wierzbowski, H., Anczkiewicz R., Bazarnik, J., Pawlak, J., 2012. Strontium isotope variations in Middle Jurassic (Late Bajocian–Callovian) seawater: Implications for Earth's tectonic activity and marine environments. Chemical Geology 334, 171–181.

Wignall, P.B., Hallam, A., 1991. Biofacies, stratigraphic distribution and depositional models of British onshore Jurassic black shales. In: Tyson R.V., Pearson T.H., (Eds.), Modern and Ancient Continental Shelf Anoxia Geological Society of London, Special Publication, London, 58, p. 291–309.

Wimbledon, W.A., 2008. The Jurassic-Cretaceous boundary: An age-old correlative enigma. Episodes 31, 423.

Wimbledon, W.A.P., Casellato, C.E., Reháková, D., Bulot, L.G., Erba, E., Gardin, S., Verreussel, R.M.C.H., Munsterman, D.K., Hunt, C.O., 2011. Fixing a basal Berriasian and Jurassic/Cretaceous (J/K) boundary – is there perhaps some light at the end of the tunnel?. Rivista ltaliana di Paleontológia e Stratigrafia 117, 295–307.

Wortmann, U.G., Weissert, H., 2000. Tying platform drowning to perturbations of the global carbon cycle with a $\delta^{13}C_{Org}$-curve from the Valanginian of DSDP Site 416. Terra Nova 12, 289–294.

Zák, K., Košťák, M., Man, O., Zakharov, V.A., Rogov, M.A., Pruner, P., Dzyuba, O.S., Rohovec, J., Mazuch, M., 2011. Comparison of carbonate C and O stable isotope records across the Jurassic/Cretaceous boundary in the Boreal and Tethyan Realms. Palaeogeography, Palaeoclimatology, Palaeoecology 299, 83–96.

Zakharov, V.A., Bown, P., Rawson, P.F., 1996. The Berriasian stage and the Jurassic–Cretaceous boundary. Bulletin de l'Institut Royal des Sciences Naturelles de Belgique, Sciences de la Terre 66, 66 (SUPPL.), 7–10.

Zeebe, R.E., Westbroek, P.A. 2003. A simple model for the $CaCO_3$ saturation state of the ocean: The "Strangelove", the "Neritan", and the "Cretan" ocean. Geochemistry Geophysics Geosystems 4(12), 1104, doi:10.1029/2003GC000538.

Ziegler, P.A., 1988. Evolution of the Arctic–North–Atlantic and the western Tethys. American Association of Petroleum Geologists Memoir 43, 30 pl.

Figures

Fig. 1. Location and palaeogeographic setting of the studied sections. A: Location of Lókút Hill and Hárskút in the Bakony Hills of the Transdanubian Range in western Hungary. B: Palaeogeographic setting of the Transdanubian Range (TR) and neighbouring units within a reconstructed Tithonian (Late Jurassic) western Tethyan palaeogeography (after Csontos and Vörös, 2004).

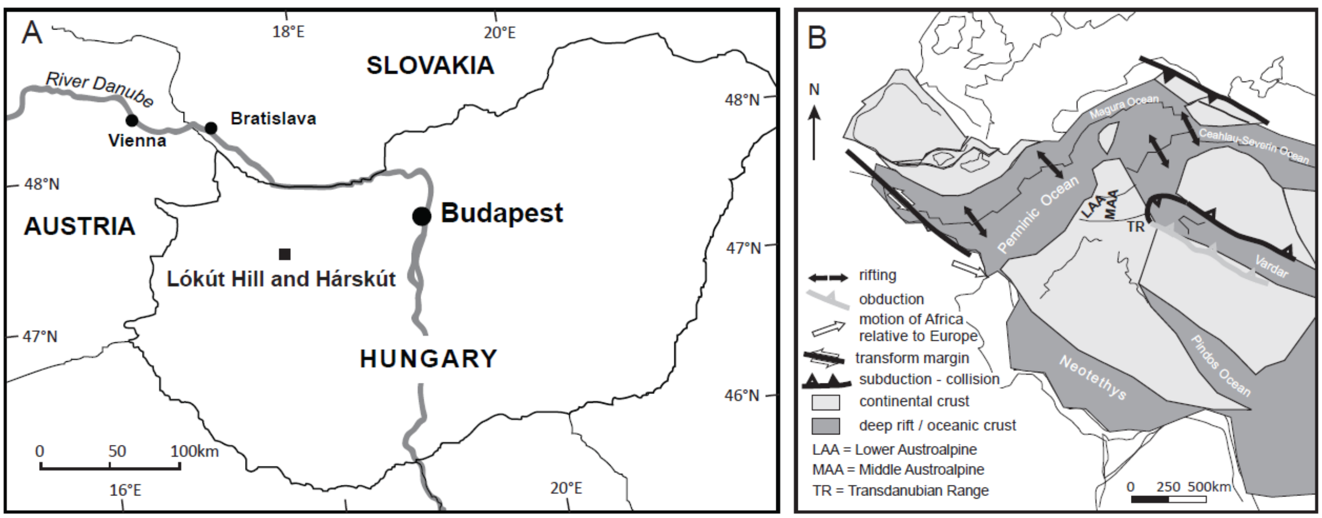

Fig. 2. Integrated biostratigraphy, magnetostratigraphy and carbon and oxygen isotope stratigraphy from the Lókút section. The measured log and samples are referenced using the bed numbers of Vigh (1984). Ammonite zones for the Kimmeridgian and Tithonian follow the zonation scheme by Enay and Geyssant (1975) and Geyssant (1997). LRF = Lókút Radiolarite Formation. Pm. = *Parastomiosphaera malmica* Zone. Belemnite assemblages are from Főzy et al. (2011).

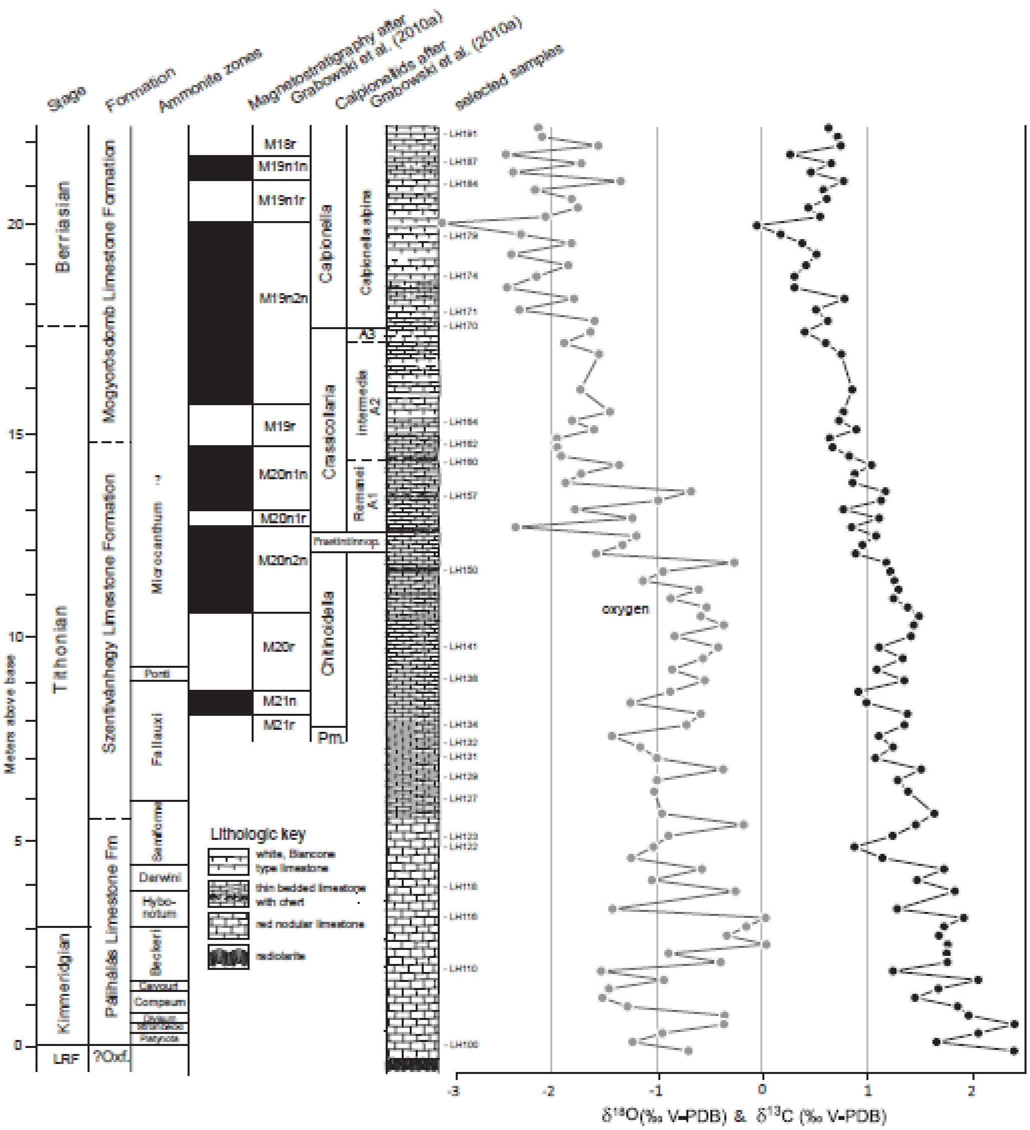

Fig. 3. Integrated stratigraphy of the Hárskút HK-II section showing the ammonite and calpionellid biostratigraphy (from Horváth and Knauer, 1986, Főzy, 1990) and carbon and oxygen isotope curves. Abbreviations: Kim. = Kimmeridgian, Occit. = Occitanica Zone; Boiss. = Boissieri Zone.

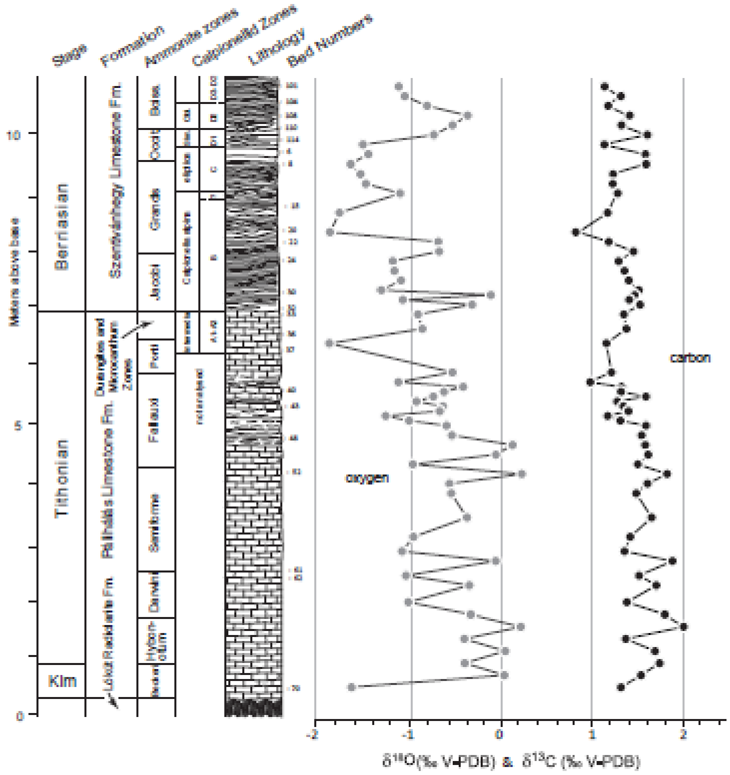

Fig. 4. Representative and age-diagnostic Late Jurassic ammonites from the Lókút section. Inventory numbers of the Department of Paleontology and Geology of the Hungarian Natural History Museum are prefixed by INV. All figures are natural size.

1. *Haploceras verruciferum* (Zittel, 1869), INV.2014.76, Bed LH 122, Semiforme Zone.

2, 3. *Simoceras biruncinatum* (Zittel, 1869), INV.2014.75, Bed LH 133, Fallauxi Zone.

4, 5. *Trapanesites adelus* (Gemmellaro, 1872), INV.2014.77, Bed LH 110-111, Compsum Zone (?).


1
2
3
4
5
1 cm

Fig. 5. Representative and age-diagnostic Late Jurassic ammonites from the Hárskút (HK-II) section. Inventory numbers of the Hungarian Geological and Geophysical Institute are prefixed by J. All figures are natural size.
1. *Haploceras verruciferum* (Zittel, 1869), J 10923, Bed 60, Semiforme Zone.
2. *Semiformiceras fallauxi* (Oppel, 1865), J 10875, Bed 54, Fallauxi Zone.
3, 4. *Haploceras carachtheis* (Zeuschner, 1846), J 10908, Bed 49, Fallauxi Zone.
5. *Semiformiceras semiforme* (Oppel, 1865), J 10870, Bed 59, Semiforme Zone.
6. *Simoceras admirandum* (Zittel, 1869), J 10965, Bed 48, Fallauxi Zone.
7. *Semiformiceras birkenmajeri* Kutek & Wierzbowski, 1986, J 10367, Bed 62, Darwini Zone.
8, 9. *Ptychophylloceras ptychoicum* (Quenstedt, 1847), J 10683, Bed 44, Fallauxi Zone.
10, 11. *Anaspidoceras neoburgense* (Oppel, 1863), J 10371, Bed 64, Darwini Zone.
12. *Haploceras elimatum* (Oppel, 1865), J 10600, Bed 51, Fallauxi Zone.
13, 14. *Lytogyroceras subbeticum* Olóriz, 1978, J 10976, Bed 42, Ponti Zone.
15, 16. *Discosphictoides* cf. *rhodaniforme* Olóriz, 1978, J 10363, Bed 59, Semiforme Zone.

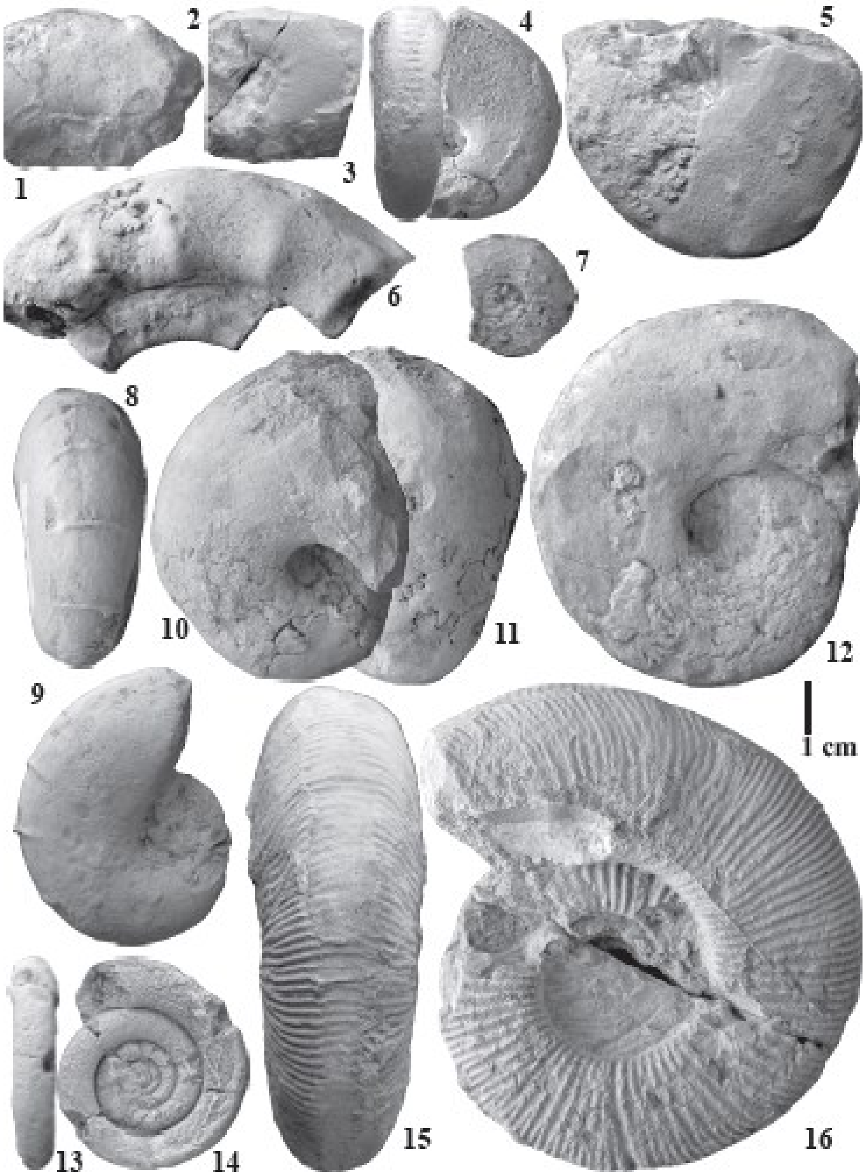

Fig. 6. Summary of global carbonate $\delta^{13}C$ correlations for the Late Jurassic-Early Cretaceous. Global correlation of $\delta^{13}C$ data is based on 31 published Late Jurassic-Early Cretaceous records from the Boreal Realm, Atlantic Ocean and Tethys. The $\delta^{13}C_{carb}$ data are from bulk sediments except for the Subpolar Urals and North Siberia composite data derived from belemnites from Dzyuba et al. (2013) and Price and Mutterlose (2004). The data from Cardador, Southern Spain (Coimbra et al., 2009) and Montclus, Vocontian Basin (Morales et al., 2013) is shown as a 3-point moving average. For each location a number is provided which corresponds to the section number in Table 1. Numeric ages (a linear scale), magnetostratigraphy and Tethyan Ammonite Zones are from GTS 2012 (Ogg and Hinnov, 2012a; 2012b).

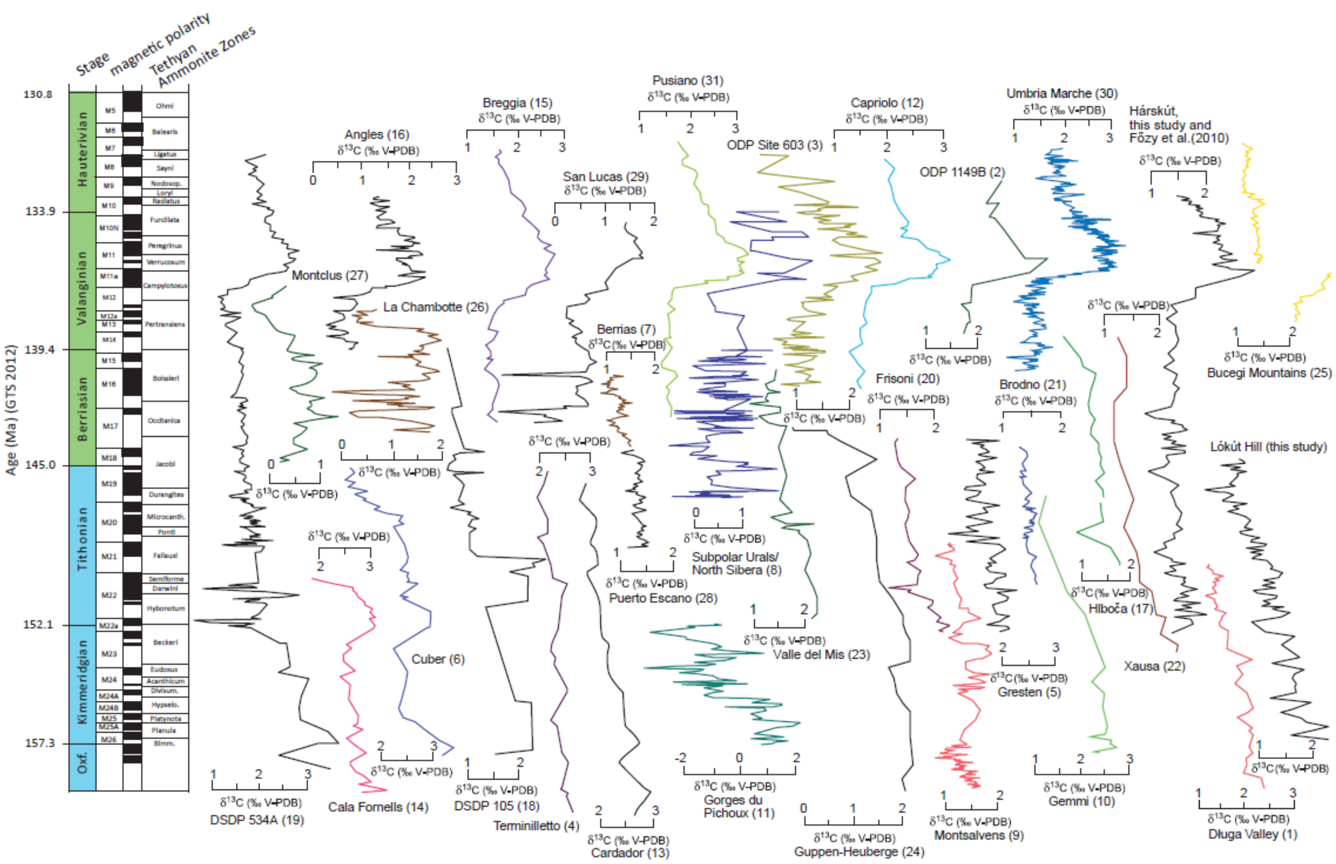

Fig. 7. Global and regional (inset) Late Jurassic palaeogeographic reconstruction (modified from Blakey, 2015) showing the distribution of localities used to generate of the $\delta^{13}C$ stack. For each location a number is provided which corresponds to the section number in Table 1. Location H = location of Hungarian sites.

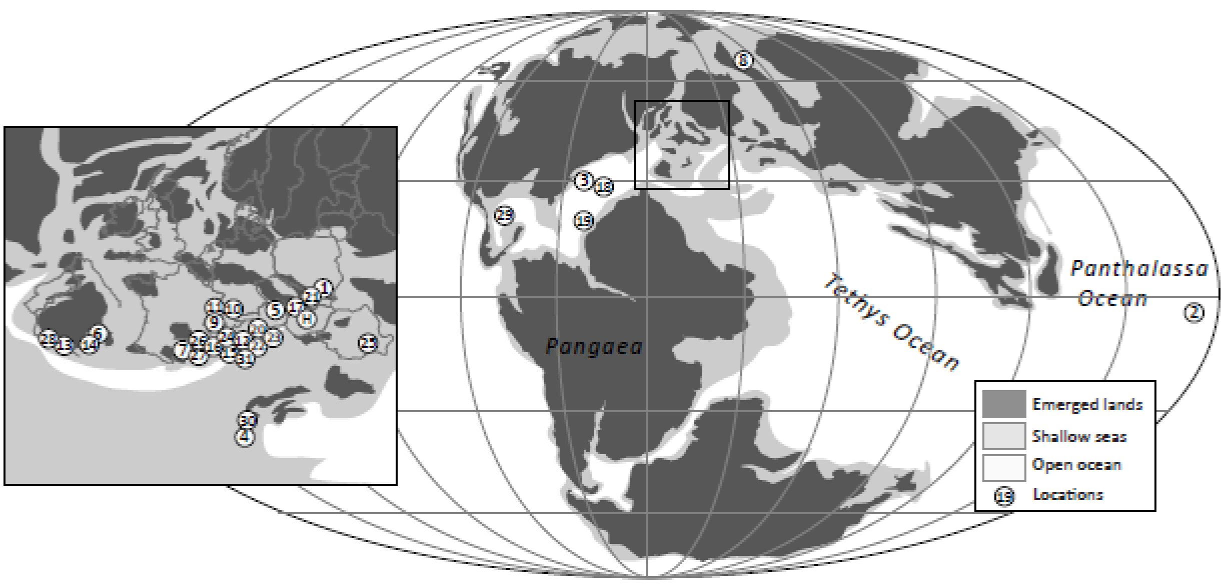

Fig. 8. A global $\delta^{13}C$ stack calibrated with magnetostratigraphy. The $\delta^{13}C_{carb}$ data are from bulk sediments as shown in detail in Fig. 6, excluding data from the Subpolar Urals and North Siberia (Dzyuba et al., 2013; Price and Mutterlose, 2004) and excluding the data from La Chambotte (Morales et al., 2013) and the Kimmeridgian data from the Swiss Jura (Colombié et al., 2011). Belemnite oxygen isotope data from sources cited within the text; the Sr isotope record from Jones et al. (1994); McArthur et al., (2004) and Bodin et al., (2009); humid and arid phases from Hallam et al. (1991) and Ruffell et al. (2002b) with Jurassic "dry event" transition phase (from Rameil, 2005) and eustatic sea-level curve from Haq (2014). Numeric ages, magnetostratigraphy and Tethyan Ammonite Zones are from GTS 2012 (Ogg and Hinnov, 2012a; 2012b).

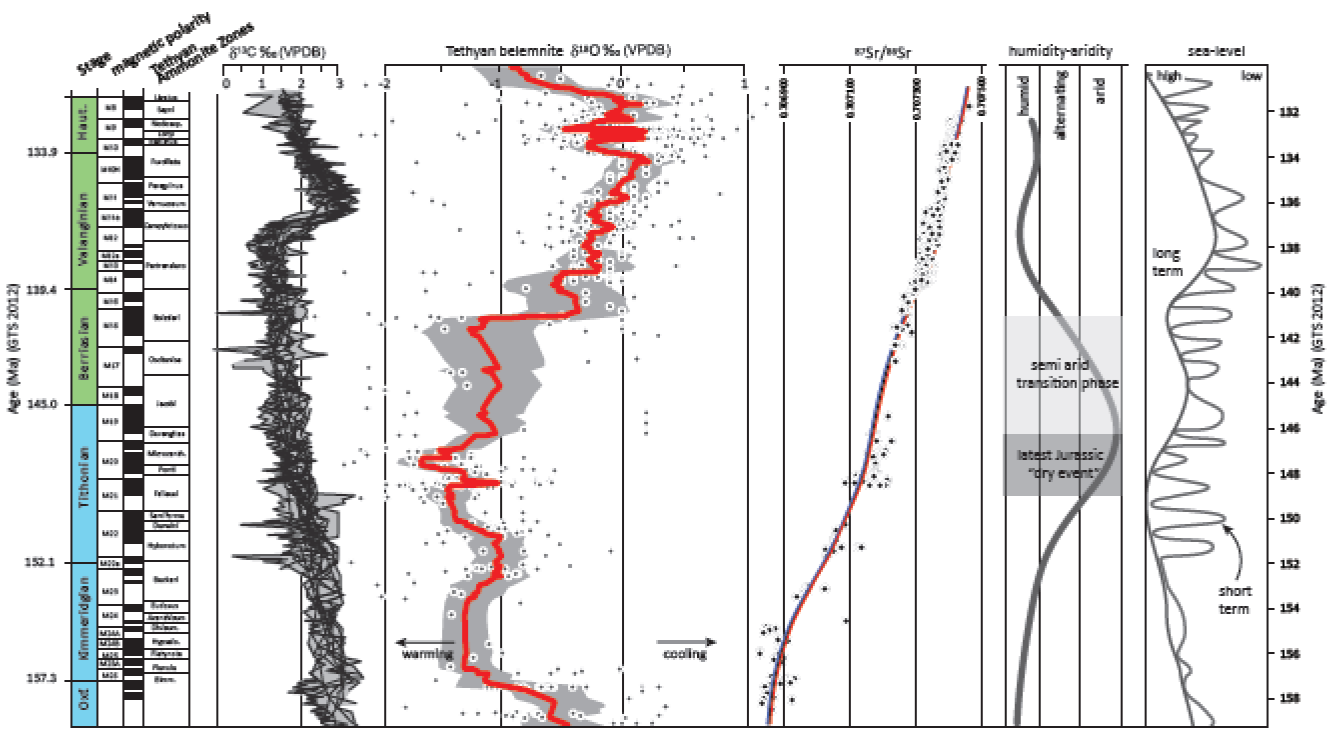

Table 1 Numbered location, stratigraphical range, magneto and/or bio-chronostratigraphic control, lithology and source reference for published Late Jurassic-Early Cretaceous carbon isotope curves.

Location	Stratigraphical span	Stratigraphic control	Lithology	Reference
1. Długa Valley, Poland	Late Oxfordian–Early Tithonian	radiolaria and calcareous dinoflagellates	nodular limestones and radiolarites	Jach et al., (2014)
2. ODP 1149B, Pacific Ocean	Valanginian–Early Hauterivian	radiolaria and calcareous dinoflagellates	radiolarian chert and nannofossil chalk and marls	Erba et al., (2004)
3. ODP Site 603, Atlantic Ocean	Late Berrisian-Early Hauterivian	nannofossils and magnetostratigraphy	nannofossil limestone and mudstones	Littler et al., (2011)
4. Terminilletto, central Italy	Late Oxfordian-Late Tithonian	radiolaria	limestone and cherts	Bartolini et al., (1999)
5. Gresten Klippenbelt, Austria	Tithonian–Early Berriasian	ammonites, calpionellids, nannofossils, magnetostratigraphy	pelagic marl-limestone cycles	Lukeneder et al., (2010)
6. Cuber, Mallorca, Spain	Late Oxfordian–Early Berriasian	ammonites	bedded and nodular marly limestones	Coimbra and Olóriz, (2012)
7. Berrias, France	Berriasian	ammonites calpionellids	pelagic limestones	Emmanuel and Renard, (1993)
8. Subpolar Urals/North Sibera	LateTithonian–Late Valanginian	ammonites, magnetostratigraphy	belemnites	Dzyuba et al., (2013); Price & Mutterlose, (2004)
9. Montsalvens, Switzerland	Late Oxfordian–Tithonian	ammonites	nodular limestones with chert	Padden et al., (2002)
10. Gemmi, Switzerland	Late Oxfordian–Tithonian	ammonites	nodular limestones with chert	Padden et al., (2002)
11. Gorges du Pichoux, Swiss Jura	Kimmeridgian–Early Tithonian	ammonites	lime mudstones	Colombié et al., (2011)

12. Capriolo, Italy	Berriasian–Hauterivian	nannofossils, magnetostratigraphy	marly limestones with chert	Lini et al., (1992)
13. Cardador, Betic Cordillera, Spain	Oxfordian–Tithonian	ammonites	bedded and nodular limestones	Coimbra et al., (2009)
14. Cala Fornells, Mallorca, Spain	Oxfordian–Early Tithonian	ammonites	bedded and nodular marly limestones	Coimbra & Olóriz, (2012)
15. Breggia, Switzerland	Berriasian–Hauterivian	nannofossils, magnetostratigraphy	pelagic limestone with chert	Bersezio,et al., (2002)
16. Angles, France	Late Berriasian–Early Hauterivian	ammonites, nannofossils, calpionellids	marl–limestone alternations	Duchamp–Alphonse et al., (2007)
17. Hlboča Slovakia	Tithonian–Early Valanginian	calpionellids, magnetostratigraphy	nodular limestone, cherty limestones	Grabowski et al., (2010b)
18. DSDP 105, Atlantic Ocean	Tithonian–Valanginian	nannofossils	limestone and claystones	Tremolada et al. (2006); Brenneke, (1978)
19. DSDP 534A, Atlantic Ocean	Early Tithonian–Hauterivian	nannofossils, magnetostratigraphy	limestone and claystones	Tremolada et al. (2006); Katz et al. (2005)
20. Frisoni, Italy	Late Kimmeridgian–Early Berriasian	calpionellids, magnetostratigraphy	nodular limestone and thin bedded limestones	Weissert and Channell (1989)
21. Brodno, Western Carpathians, Czech Republic	Tithonian–Early Berriasian	Calpionellids, nannofossils, magnetostratigraphy	pelagic limestones	Michalik et al., (2009)
22. Xausa, Italy	Late Kimmeridgian–Berriasian	calpionellids, magnetostratigraphy	nodular limestone and thin bedded limestones	Weissert and Channell (1989)
23. Valle del Mis, Italy	Tithonian–Early Berriasian	calpionellids, magnetostratigraphy	nodular marly limestone and thin bedded limestones	Weissert and Channell (1989)
24. Guppen – Heuberge, Switzerland	Late Oxfordian–Early Berriasian	ammonites, calpionellids	nodular and micritic limestones	Weissert and Mohr, (1996)
25. Bucegi	Early Valanginian–	ammonites,	pelagic limestones	Barbu,

Mountains, Romania	Early Hauterivian	nannofossils		(2014)
26. La Chambotte, France	Early Berriasian–Early Valanginian	foraminifera, calpionellids,	shallow-water limestones	Morales et al., (2013)
27. Montclus, France	Early Berriasian–Early Valanginian	ammonites, nannofossils	hemipelagic marl-limestones	Morales et al., (2013)
28. Puerto Escano, Spain	Tithonian–Early Berriasian	calpionellids, ammonites, magnetostratigraphy	limestones and nodular limestones	Zak et al., (2011)
29. San Lucas, Mexico	Berriasian–Valanginian	calpionellids	Marls and limestones	Adatte et al., (2001)
30. Umbria, Italy	Berriasian–Hauterivian	calpionellids, magnetostratigraphy	limestones	Sprovieri et al., (2006)
31. Pusiano, Northern Italy	Berriasian–Hauterivian	Nannofossils, magnetostratigraphy	Pelagic limestones	Channell et al., (1993)